Highquest Engineering Inc.

THERMALLY COUPLED PRESSURE SWING ADSORPTION FOR NATURAL GAS CONVERSION TO LIQUID FUELS

Final Report

by

Principal Investigator:		B.G.Keefer
Consultant	:	D.M.Ruthven
Research Assistants	:	G.D.Lepp, M.G.Chew
Address	:	Highquest Engineering Inc. 516-675 W. Hastings St. Vancouver, B.C. V6B 1N2

Work on this project was conducted under the auspices of the Canada Centre for Mineral and Energy Technology, Energy, Mines and Resources, Canada.

DSS FILE NUMBER : 15SQ.23440-5-9144

DSS CONTRACT SERIAL NUMBER : OSQ85-00131

CANMET PROJECT NUMBER : 503111

CANMET SCIENTIFIC AUTHORITY: Dr. D.D.S. Liu

July 1986

This report should be cited as Contract Report No. OSQ85-00131

100 pp

MICROMEDIA

TABLE OF CONTENTS

LIST OF FIGURES		ii
LIST OF TABLES		iv
1.0	EXECUTIVE SUMMARY	2
2.0	SUMMARY OF WORK ACHIEVED	3
2.1	Task A1 - Preliminary Theoretical Modelling	3
2.2	Task A2 - Identification of Adsorbents	3
2.3	Task A3 - Experimental Design	4
2.4	Task A4 - Experimental Facilities	4
2.5	Task A5 - Experimental Investigations	4
2.6	Task A6 - Interpretation and Analysis of Results	5
3.0	THEORETICAL INVESTIGATIONS	6
3.1	Background	6
3.2	TCPSA Reactor Principles	9
3.3	Steam Reforming Process Considerations	12
3.4	Stirling Cycle Modelling	14
3.5	Adsorption Equilibrium Model	17
3.6	Allowance for Adsorbent Rate Effects	19
3.7	Heat and Material Balances	20
3.8	Physical Size Estimates	24
4.0	SELECTION OF ADSORBENTS	25
5.0	EXPERIMENTAL INVESTIGATIONS	27
5.1	Adsorbent Selectivity Experiments	27
5.2	TCPSA Apparatus	28
5.3	Procedure	30
5.4	Results	31
6.0	ANALYSIS AND INTERPRETATION OF RESULTS	34
7.0	CONCLUSIONS AND RECOMMENDED FUTURE WORK	36
FIGURES		37
ANNEX A	- References	A1
ANNEX B	- Development of Equilibrium Theory for TCPSA Separations	B1
ANNEX C	- Experimental Run Log	C1
ANNEX D	- Stirling Cycle Analysis	D1

LIST OF FIGURES

Figure 1	-	Methane to Gasoline Reaction Pathways	37
Figure 2a	-	P-V and T-S diagrams for an Ideal Stirling Cycle	38
Figre 2b	-	Typical Piston Motions for an Ideal Stirling Cycle	38
Figure 3	-	Directions of Heat and Mass Transport in a basic "TCPSA" module.	39
Figure 4	-	Schematic of a "TCPSA" Methane To Liquid Fuel Converter	40
Figure 5	-	Schematic of TCPSA Reactor	41
Figure 6	-	Pressure and Mass Flows vs Crank Angle for a Typical Modelling Run of the Compound Stirling Cycle TCPSA Reactor	42
Figure 7	-	Isosteres of H_2O on 4A Molecular Sieve	43
Figure 8	-	Isosteres of H_2O on Silica Gel	44
Figure 9	-	Isosteres of H_2O on Silicalite, NaX and Aluminophosphate Molecular Sieves (Ref. W1)	45
Figure 10	-	Extrapolated Isosteres of H_2O on Silicalite	46
Figure 11	-	Adsorption Equilibrium Coefficients vs Temperature for Silicalite	47
Figure 12	-	Adsorption Equilibrium Coefficients vs Temperature for Alcan Alumina	48
Figure 13	-	Adsorption Equilibrium Coefficients vs Temperature for Ultra Stable Y Zeolite	49
Figure 14	-	Schematic of the Highquest TCPSA test rig	50
Figure 15	-	Photograph of the Highquest TCPSA test rig	51
Figure 16	-	Photograph of the Highquest TCPSA test rig	52
Figure 17a	-	Chromatograph configuration. Sample valve open and columns A and B in series with the TCD	53
Figure 17b	-	Injection of the sample. Column A inline with the TCD, column B off-line.	53

Figure 17c - Injection of the sample, columns A and B in series with the TCD. 53

Figure 18 - Chromatogram of Run #040886-05. Components N_2, H_2O 54

Figure 19 - Chromatogram of Run #041086-01. Components N_2, H_2O 55

Figure 20 - Chromatogram of Run #041186-01. Components N_2, H_2O 56

Figure 21 - Chromatogram of Run #041886-01. Components N_2, H_2O 57

Figure B1 - Flow - Controlled PSA Cycle. Normal Type I B16

Figure D1 - Schematic for Stirling cycle analysis nomenclature D3

LIST OF TABLES

Table C1	-	Summary of Experimental Run Conditions and Results	C2
Table D1	-	Beta Stirling Engine/Heat Pump analysis	D12

1.0 EXECUTIVE SUMMARY

This document outlines the results obtained from work performed to conduct an initial assessment of Highquest's Thermally Coupled Pressure Swing Adsorption (TCPSA) process for converting natural gas into liquid fuels, with experimental attention to the steam reforming step.

Work under this contract included preliminary theoretical modelling, investigation of candidate adsorbents, and experimental tests of gas separation under steam reforming conditions. Experiments were conducted to measure adsorbent selectivities directly in a heated gas chromatograph column, while successful high temperature steam separation was demonstrated using Highquest's experimental TCPSA test rig.

Positive results were obtained from the reported work, whose limited objectives were to show the feasibility of steam separation from a mixture of methane and synthesis gas components at the high temperatures expected in a TCPSA steam reformer. Theoretical models were developed, and correlated to experimental results. Quantitative adsorption selectivity data were obtained for three selected candidate adsorbents, using a heated chromatographic column. The most suitable adsorbents were found to be alumina and ultra-stable Y zeolite, subject to further investigation of their long term stability under severe hydrothermal conditions. Highquest's experimental TCPSA test rig was operated using alumina adsorbent, achieving satisfactory separation of steam from nitrogen at temperatures ranging up to 800° Celsius. Results demonstrate the scientific feasibility of TCPSA, and are encouraging toward eventual commercial feasibility.

This report presents the theoretical and experimental methodology and results that indicate the feasibility of separating steam at high temperature from other syngas reaction constituents. The experimental results are applied within the theoretical framework to indicate physical and performance parameters of a projected pilot scale process, and to identify areas of risk or uncertainty.

2.0 SUMMARY OF WORK ACHIEVED

2.1 Task A1 - Preliminary Theoretical Modelling

1. A critical review of prior art processes and the proposed process was conducted in order to identify critical issues affecting feasibility and future optimization.

2. Stirling cycle modelling was conducted for the proposed coupled TCPSA heat pump reformer and exothermic Fischer-Tropsch syngas converter. The idealized "Schmidt model" for the corresponding heat pump and engine cycles was programmed on a small computer, and numerous runs were made for different selections of phase angle parameters to define heat balances, mass flows, and pressure ratios for operating regimes consistent with PSA separation criteria.

3. An equilibrium model of adsorptive separation was developed for a basic TCPSA cycle, and used to derive idealized separation criteria correlated to the Stirling cycle model. This equilibrium model is generalized from prior references in order to accommodate the novel TCPSA feature of independent control of pressure and flow direction by pistons, and also by the inclusion of axial dispersion effects.

4. Modification of optimal phase relationships between the cyclic pressure and mass flows over the adsorbent was analyzed, using heat transfer analogies to model diffusive transport within the adsorbent.

5. Heat and material balances were calculated for steam reforming and syngas conversion reactors. Alternative approaches to providing supplemental heat were considered.

6. Preliminary estimates were made for reactor physical proportions for assumed liquid fuel production of 50 bbl per day.

2.2 Task A2 - Identification of Adsorbents

1. A literature search on adsorbents and steam reforming technology was conducted.

2. Expert advice was obtained on adsorbent selection from D.M. Ruthven of UNB, and from R. Anderson and G. Keller of Union Carbide.

3. Three adsorbents (alumina, silicalite and ultrastable Y zeolite) were selected for the experimental work. Alumina and silicalite were obtained in 1/16" pellet form, while the ultrastable Y (cracking catalyst) was available only as powder.

4. Pending experimental results, a preliminary theoretical extrapolation was made of adsorbent selectivities into the regime of high temperatures and high steam partial pressure.

2.3 Task A3 - Experimental Design

1. An adsorbent housing was fabricated for the Highquest TCPSA test rig, with provision for sampling from the two ends (hot and cold) of the housing.

2. The test rig was assembled and prepared for initial test operations, using a modified industrial oven for heating the apparatus.

2.4 Task A4 - Experimental Facilities

A gas chromatograph, furnace and other laboratory equipment were procured and prepared for combined operation with the test rig.

2.5 Task A5 - Experimental Investigations

1. Professor Ruthven's group at UNB conducted a series of high temperature adsorption tests in a heated gas chromatograph column using steam reforming gas components and steam over each of the three selected adsorbents (silicalite, alumina and ultrastable Y zeolite) in direct support of Highquest's program. This activity corresponded to the initial work plan of Highquest's proposal, and yielded valuable quantitative data complementing the more qualitative results obtained directly from the TCPSA test rig.

2. The Highquest TCPSA test rig was operated at low temperatures with syngas over 13X zeolite (demonstrating

hydrogen separation as expected, but failing to show clear separation of water owing to excessive loading of the adsorbent), and at high temperatures with nitrogen and steam. The high temperature experiments were performed with alumina adsorbent, working in a batch mode aimed to concentrate an initial injection of water from one end of the adsorbent column to the other end. Satisfactory qualitative results were obtained, as discussed in Section 5 below.

2.6 Task A6 - Interpretation and Analysis of Results

The qualitative data obtained using the Highquest test rig show that steam can be separated effectively under steam reforming conditions. The quantitative data obtained at UNB was applied to Highquest's theoretical model in order to confirm the ability of a projected full scale TCPSA steam reformer to achieve full water separation from its syngas effluent while operating at full capacity. All results obtained are consistent with prospective feasibility of the proposed process, although many practical issues such as adsorbent stability have been insufficiently addressed.

3.0 THEORETICAL INVESTIGATIONS

3.1 Background

This contract was aimed at achieving a preliminary feasibility investigation into some aspects of unconventional processes for directly converting natural gas into liquid fuels. This process development may achieve improved energy efficiency and process simplifications leading to economically attractive conversion of natural gas to liquid fuels, particularly high octane gasoline.

The key ingredient of the process technology is an unconventional reactor using the new principle of "thermally coupled pressure swing adsorption" (TCPSA), in which the heat recovery and product separation subsystems are directly integrated with the reactor. To achieve this, the TCPSA reactor integrates the known pressure swing adsorption (PSA) separation process with a Stirling cycle machine which achieves the heat recovery. The Stirling cycle machine achieves the heat recovery through conversion of heat to work or vice versa; and operates on a closed regenerative thermodynamic cycle, with cyclic compression and expansion of the working fluid at different temperature levels, and with flow controlled by volume changes. In the case of a TCPSA reactor, the Stirling cycle (using the reactant and product gases as working fluid) transports and converts heat of reaction as heat of compression (endothermic) or expansion (exothermic). It also generates an appropriate regime for cyclic pressure and flow oscillations over an "adsorbent regenerator" to separate the product and reactant gas species. The adsorbent regenerator has the combined functions of heat storage (the Stirling cycle regenerator) and selective adsorption of gas components (the PSA adsorbent bed).

The TCPSA principle applies to gas or vapour phase chemical reactors where separation and heat conversion effects both go in the right direction, and also to non-reactive gas separations (such as an air separation using waste heat to generate oxygen for high temperature processes).

The TCPSA reactor offers potential advantages of energy efficiency and process simplification by integrating heat recovery and product separation elements. TCPSA may be particularly advantageous for reactions with severe equilibrium constraints, with problems in conversion or selectivity performance, or with heat transfer difficulties.

The TCPSA reactor and gas separation systems have been conceived as general tools for future chemical process development. In some cases they may improve the economics of established processes, and in other cases possibly pulling presently uncompetitive reaction pathways (such as partial oxidation of methane to methanol) into economic contention.

In addressing the challenge of converting natural gas into liquid fuels (as directly as possible but, above all, economically), TCPSA may be applied to any of several reaction pathways or, in principle, to any new gas phase reactions that might emerge from catalyst research groups elsewhere.

The following reaction pathways are recognized at present (see also Fig. 1.):

1. steam reforming of methane to syngas, and Fischer-Tropsch conversion of syngas to liquid hydrocarbons, with optional use of shape selective zeolite with F-T catalyst to achieve high selectivity (references C1, C2, C3, D1, L1 and S1);

2. steam reforming of methane to syngas, conversion of syngas to methanol, and methanol to gasoline conversion over shape selective zeolite (Mobil MTG process, reference C3);

3. high temperature partial oxidation of methane to syngas (reference S2), followed by Fischer-Tropsch (F.T.) conversion;

4. partial oxidation of methane to syngas followed by conversion to methanol and MTG conversion to gasoline;

5. controlled partial oxidation of methane to methanol (references F3, H1 and H2), followed by MTG conversion to gasoline.

In principle, the TCPSA concept may be applied to each step of each process pathway above, with further possibilities of coupling the TCPSA reactors of each step to achieve efficient energy transfer, process simplification and economic benefits.

It may be noted that high temperature partial oxidation (POX) of methane to syngas is a typically non-catalytic process normally conducted at about 1400 degrees C, with an oxygen to natural gas ratio of about 0.7 (see pages 118-121 of reference S2). While POX is well established for gasification of heavy hydrocarbon feedstocks and coal, steam reforming has dominated the commercial conversion of methane and other light hydrocarbons to syngas. The considerably lower capital cost of a POX reactor compared to a steam reformer has been more than offset by the cost of purchased oxygen. Lower cost of oxygen could shift the economic balance in favour of POX for natural gas conversion (see reference M1). TCPSA thermally powered air separation modules may perhaps reduce the future cost of process oxygen, by applying the exothermic POX reaction heat as the primary energy source for air separation as disclosed in reference K2.

Highquest plans to examine these alternatives in its development program, and so select the best chemical pathway optimized in the TCPSA context. The present project had the more restricted mandate of investigating applicability of TCPSA to the steam reforming based pathways, with experimental focus on selectivity under steam reforming conditions in a TCPSA test rig.

3.2 TCPSA Reactor Principles

As mentioned in Section 3.1, the Stirling cycle is a closed, regenerative thermodynamic cycle which cyclically compresses and expands a working fluid at different temperature levels, and in so doing converts heat to work or vice versa, depending on whether the cycle is operated as an engine or a heat pump respectively.

An ideal Stirling cycle engine can be represented by a closed volume containing two opposed cylinders and pistons (Figure 2). Between the pistons is a thermal regenerator which alternatively absorbs and releases heat. The motion of each of the pistons defines a variable volume space in the corresponding cylinder. The variable volume space whose displacements have leading phase (with repect to the other variable volume space) is called the expansion space, and the lagging variable volume space is called the compression space.

For operation as an engine converting heat to mechanical work, the expansion space is maintained at an elevated temperature with respect to the compression space. The cycle illustrated in Figure 2b begins with the pistons in configuration (1) travel corresponding to point 1 on the P-V and T-S diagrams in Figure 2a. The compression piston then moves to the left performing an isothermal compression until point 2 is reached. During compression, heat is transferred from the working fluid to the surroundings, mostly at the temperature of the compression space which contains most of the gas. Next, both pistons move to the left in a constant volume process, transferring the gas to the hot end and transferring heat from the regenerator to the working fluid. From points 3 to 4 only the expansion piston moves, performing an isothermal expansion while heat is transferred to the working fluid from an external source at the temperature of the expansion space. The final step from 4 to 1 is another constant volume shift in which heat is transferred from the working fluid to the regenerator. The net effect of the cycle is to transport heat across the temperature gradient from expansion space to compression space, and convert part of the heat to work according to the temperature ratio.

For operation as a heat pump, the Stirling cycle is operated in the reverse direction. The expansion space becomes the cooler end, and the compression space the warmer end. External work must be performed on the system to move the heat from the expansion space to the compression space.

In the case of a TCPSA reactor (reference K2), the regenerator is integrated with an adsorbent bed. A catalyst bed may be associated with the variable volume space of the Stirling cycle providing the appropriate heat sink (exothermic reaction) or heat source (endothermic reaction) for the process. The cyclic pressure and flow variations of the Stirling cycle provide the necessary regime for PSA separation in the adsorbent loaded regenerator. Exothermic reactions are conducted in the expansion space which provides a direct heat sink (without external heat exchangers), while conversely endothermic reactions can be conducted in the compression space whcih provides the appropriate heat source. The TCPSA reactor concept is shown in Figure 5.

While the Stirling cycle transports heat from the expansion space to the compression space, the more readily adsorbed components of the working fluid gas mixture will also be transported toward the compression space while the less readily adsorbed components will be transported toward the expansion space. This follows from the fact that the working fluid flows toward the expansion space at relatively high pressure (immobilizing the more readily adsorbed components on the adsorbent, and concentrating the less adsorbed fraction toward the expansion space), while the reverse flow toward the compression space occurs while the pressure is reduced. Thus the more readily adsorbed fraction is mobile and is preferentially concentrated to the compression space. Hence, a TCPSA system transports heat and preferentially adsorbed gas components in the same direction as shown schematically in Figure 3, while the less adsorbed gas components are transported in the opposite direction.

TCPSA may have application to any given reaction process, where there is a candidate adsorbent providing a clearly defined separation which pulls desired reaction products out of the reaction zone and pushes reactants and any undesired side reaction products in. The adsorptive separation must drive reaction equilibrium in a useful direction, consistent with conversion and selectivity objectives. The direction of the separation must also be consistent with the direction of Stirling cycle heat transport, with exothermic reactions normally conducted in the expansion space and endothermic reactions normally conducted in the compression space.

Steam reforming is an endothermic reaction, in which steam (usually readily adsorbed) should be concentrated over a heated catalyst. It is consistent with TCPSA transport of heat and the

more adsorbed components in the same direction. Fischer-Tropsch synthesis is an exothermic reaction, whose desired products are more readily adsorbed than the syngas reactants, again consistent with the basic TCPSA functions. Hence, the TCPSA concept seems potentially applicable to both steam reforming and F.T. stages of a natural gas to liquid fuel conversion process. Since the product syngas of the steam reformer is the feed to the F.T. converter, the separate TCPSA stages may be cascaded into a combined plant as shown schematically in Figure 4. Part of the exothermic heat of the F.T. stage of the Figure 4 combined system can then be directly applied to the expansion end of the steam reforming stage, and then raised by heat pumping action up to steam reforming temperatures as a contribution to the endothermic heat requirement.

3.3 Steam Reforming Process Considerations

In the conventional approach to steam reforming, a highly endothermic reaction is conducted at relatively high pressure contained by highly stressed catalyst tubes. Technical and economic constraints are:

- tubes operate near their metallurgical limit. Costly alloys must be used, and periodic replacement is necessary;
- considerable excess of steam is necessary (at high energy cost) to drive the equilibrium toward high methane conversion and to inhibit carbon deposition on the catalyst;
- high heat flux through the tubes results in large temperature drops between the furnace and the catalyst;
- heat transfer considerations and need for low pressure drop in long catalyst tubes require large catalyst pellets in order to obtain sufficient void volume. Catalyst effectiveness is consequently very low (about 10%).

These factors mean that the majority of both capital costs and energy losses of a natural gas fed methanol plant are concentrated in the steam reforming section of the plant (reference M1). There is much room for improvement.

In the TCPSA steam reformer concept, heat is provided at least in part by Stirling cycle heat pumping from a lower temperature heat source such as the exothermic syngas converter. This reduces, and may eliminate the heat transfer conduction load through the catalyst tubes or containment vessel. A more favourable catalyst geometry (with smaller pellets) may be used to improve effectiveness. If all the endothermic heat of reaction is supplied internally as Stirling cycle heat of compression, required heat conduction load becomes zero and exotic metallurgy of the pressure vessel may be avoided. However, the design of the catalyst bed and displacer for optimal compression heat transfer to the catalyst presents considerable challenges as well as opportunities.

The TCSPA steam reformer is intended to concentrate and trap steam at its hot end as water vapour will be selectively adsorbed (even at high temperatures) by a suitable adsorbent. If steam is totally separated from the syngas effluent leaving the cooler end of the reformer, it need only be supplied at the

stoichiometric rate. A high partial pressure of steam can be maintained over the catalyst, driving the equilibrium from methane toward syngas, and preventing carbon deposition on the catalyst. A change in the steam/carbon ratio from 2 to 6 shifts the equilibrium corresponding to a temperature increase of over 100 degrees Celsius.

The effective steam/carbon ratio can be changed by adjusting the rate of steam admission, providing a means of control.

High steam concentration also drives the water gas shift reaction toward CO_2. If the TCPSA adsorbent has significant selectivity under working conditions for CO_2 as well as water, CO_2 will be trapped to some extent over the steam reforming catalyst, pushing the shift reaction back toward CO_2 production, and retarding the overall rate of reaction somewhat. As usual Fischer-Tropsch catalysts have low activity for the shift reaction (e.g. compared with methanol synthesis catalysts), the syngas composition should be shifted toward carbon monoxide upstream of F-T synthesis.

Technical risk areas in the development of a TCPSA steam reformer include:

1. possible inadequate hydrothermal stability of adsorbent;

2. possible mechanical breakdown of adsorbent or catalyst under cyclic operating conditions (however, durability of catalysts under large amplitude temperature swings in cyclic reformers is established).

3. impaired energy conversion efficiency of the Stirling cycle owing to dissipation effects withion the adsorbent bed and static heat conduction losses.

3.4 Stirling Cycle Modelling

Modified Stirling cycle machines operating in the high temperature heat pump function for steam reforming and the lower temperature engine function for syngas conversion were modelled using the assumptions of the "Schmidt model" discussed for example in reference U1.

The Schmidt model is a first order approximation of the ideal Stirling cycle, with the following assumptions:

1. the regenerative process is perfect (infinite heat capacity of regenerative matrix, and perfect heat transfer).

2. the instantaneous pressure is the same throughout the system.

3. the working fluid is an ideal gas.

4. there is no leakage, and the cycle is closed to any external transport of working fluid.

5. the volume of the working spaces (compression and expansion spaces) vary sinusoidally.

6. temperatures of cylinder walls, pistons and heat exchange surfaces are constant with time.

7. temperature of the working fluid is constant at each location within the closed system.

8. there is perfect mixing within compression and expansion spaces.

9. the machine operates at constant speed, and steady state conditions have been established.

Using these approximations, the equation of state for an ideal gas is used with the expressions for variations of working space volume as functions of crank angle or time, and applied to derive an expression for pressure variation in the machine as a function of crank angle.

In this approximation, all processes at each point of the machine are isothermal, and the instantaneous pressure at each point is the same, i.e. there is no flow friction. The total number of

moles of free gas is constant, so adsorption and chemical reaction effects must be approximated as extra dead volume. Volume displacements are imposed kinetically as sinusoidal piston motions with specified amplitudes and phases. Temperature and dead volume distributions are specified. Pressure, mass flows and power at each instant are calculated by integration of the ideal gas law. This model is a reasonable first approximation for the present case of low cyclic speed and likely low adsorbent capacity under steam reforming conditions.

While the present contract was concerned primarily with the steam reforming step, it was assumed in the model that the exothermic heat of the F.T. reactor would be supplied directly to the cool end of the TCPSA steam reformer. Some of this heat would be carried by Stirling cycle heat pump operation to the hot end of the steam reformer, while the balance of heat is applied in this model as thermal power (through an integrated Stirling cycle engine) to drive the heat pump. Hence the F.T. reaction (whether or not operated in the TCPSA mode) can provide thermal power to the high temperature steam reforming TCPSA reactor.

The model was programmed on an IBM PC computer. For an arbitrary allocation of dead volumes and displacement amplitudes, the two independent phase angles were varied with increments of 10 degrees for a total of 36 X 36 = 1296 runs. Only those runs meeting the following criteria were considered further:

1. heat delivered at hot end (to endothermic reforming reaction)

2. heat accepted at intermediate temperature (from exothermic syngas conversion reaction)

3. mass flow in steam reformer regenerator (positive towards colder end) in phase with pressure, or lagging slightly (say 20 degrees) behind pressure

4. ratio of maximum to minimum pressure as high as possible within above constraints

5. total mechanical work generated slightly positive (to overcome losses and enable self-sustaining operation.

Condition (3) above is necessary to achieve proper pressure swing adsorption function. A slight lagging phase will allow for diffusive mass transfer into the adsorbent material, which will be fast in the steam reforming section.

Figure 6 shows results for a typical run satisfying the above criteria. These results indicate basic thermodynamic compatibility of the coupled heat pump and engine Stirling cycles, and consistency with the adsorption separation function in the TCPSA steam reformer. For this run, the temperatures shown in Figure 4 were assumed for steam reforming, F.T. heat recovery and heat rejection. Reference piston diameters for laboratory scale TCPSA steam reformer and F.T. heat recovery modules were set at 5 cm, with a stroke of 10 cm for each piston. Dead volume associated with steam reforming, F.T. heat recovery and heat rejection zones was taken as 150 cc for each zone. Operating speed was taken as 10 rpm, and maximum working pressure was taken as 10 atm. Excess work generated by the F.T. heat recovery "engine" is applied to drive the TCPSA steam reforming "heat pump". The phase angles between expansion and compression pistons of both "engine" and "heat pump" modules were adjusted to obtain the Figure 6 results (which show consistency of flow and pressure phase relationships to perform PSA separation in each module), while also obtaining the following data for heat and work generated per cycle, using the Schmidt model simulation of the combined system:

- Heat delivered to steam reforming catalyst: -33.94 Joules
- Heat lifted from syngas conversion catalyst: 60.58 Joules
- Heat rejection to ambient: -26.17 Joules
- Net work to help overcome friction losses: 0.47 Joules

These calculated values of heat flow and net work are used in Sections 3.6 and 3.7 to examine heat balances for the combined steam reforming and syngas conversion system, and to project the physical proportions of a pilot scale plant.

Future work will include more elaborate Stirling cycle models incorporating dynamic response of the adsorbent, and all significant thermodynamic and fluid flow loss mechanisms. Static heat conduction will be a large and perhaps dominant contributor to losses from the ideal Stirling cycle for this very low speed process.

3.5 Adsorption Equilibrium Model

An adsorption separation model was developed, based on the following assumptions:

1. linearity of isotherms
2. locally isothermal conditions on adsorbent bed
3. two component mixture (for steam reforming, water is adsorbed and all other components may be lumped together as inert)
4. instantaneous constant pressure at all points
5. rate effects neglected, i.e. adsorbent is at equilibrium with contacting mixture
6. axial dispersion term retained in certain calculations requiring estimate of mass transfer zone width.

Annex B documents the model. Similar models have been reported in the literature (see references F1 and K3). The model was applied to develop separation performance criteria for a single bed PSA device operated in accordance with the idealized Stirling cycle. These criteria reduce to:

1. flow displacement vs bed height for design productivity of fully dehydrated syngas (steam concentration characteristics entering the bed are fully rejected back to hot end)
2. no breakthrough of steam concentration characteristics (penetrating entire bed height in one cycle).

For the widely applicable case of a two component mixture with the more strongly adsorbed component present in arbitrary amounts, the model gives closed form solutions. These solutions are based on the prescribed motion of both hot and cold pistons, or on the motion of either piston with prescribed pressure changes, as control variables.

The above separation criteria were correlated to the input and output data of the Stirling cycle model to yield a target for adsorbent dynamic capacity. The effect of the adsorbent on the Stirling cycle was accomodated simply as an extra allowance for

dead volume in the regenerator. This first order approximation is reasonable when adsorptive capacities are relatively low, as expected for high temperature steam reforming. It was concluded that this capacity (slope of isotherms) for steam should be at least

$$0.2 \ \frac{\text{mmole } (H_2O)}{\text{g . atm}(H_2O)}$$

and preferably

$$0.5 \ \frac{\text{mmole } (H_2O)}{\text{g . atm}(H_2O)}$$

referenced to adsorbent weight (g) and steam partial pressure (atm), under typical steam reforming conditions (adsorbent working temperature 700 K to 1000 K, and average steam partial pressure range 1 atm to 20 atm). The corresponding range of dimensionless adsorbent loading equilibrium coefficents "K" (defined in Annex B) is approximately $10 < K < 50$, where K is the ratio of concentration in the adsorbed phase to concentration in the gas phase, with concentration expressed in the same units.

The dynamic capacity parameters of actual adsorbents will determine the feasible range of operating conditions for a TCPSA steam reformer, which may be restricted relative to previous practice for conventional reformers.

3.6 Allowance for Adsorbent Rate Effects

In the limit of equilibrium and isothermal conditions, best adsorptive separation by "parametric pumping" action will be achieved when pressure and flow swings are in phase. Optimal phase relationships are modified by mass transfer delays and possible kinetic selectivity. In the absence of kinetic selectivity effects, diffusive mass transfer limitations can cause a lag of up to 45 degrees in the optimal phase of flow relative to pressure. This is precisely analogous to heat conduction in a solid slab with periodic boundary temperature conditions (reference G2). It is assumed here that adsorbent selectivity is based on equilibrium rather than kinetic effects in the steam reforming regime, which is plausible as all physical adsorption rates should be fast at high temperatures.

3.7 Heat and Material Balances

Steam reforming reactions are:

$$CH_4 + H_2O \rightarrow CO + 3\ H_2$$

@ 298 deg. K (ΔH_{298} = 206.3 KJ/mole)
@ 1000 deg. K (ΔH_{1000} = 225.6 KJ/mole)

$$CH_4 + 2\ H_2O \rightarrow CO + 4\ H_2$$

@ 298 deg. K (ΔH_{298} = 165.1 KJ/mole)
@ 1000 deg. K (ΔH_{1000} = 190.5 KJ/mole)

$$CO + H_2O \rightarrow CO_2 + H_2$$

(ΔH_{298} = -41.2 KJ/mole)

A typical syngas effluent from steam reforming may have equal concentrations of carbon monoxide and dioxide,

$$CH_4 + \frac{3}{2}\ H_2O \rightarrow \frac{1}{2}\ CO + \frac{1}{2}\ CO_2 + \frac{7}{2}\ H_2$$

Syngas conversion reactions (with heat of reaction per mole of carbon) include

n- heptane

$$CO + \frac{15}{7}\ H_2 \rightarrow \frac{1}{7}\ n\text{-}C_7H_{16} + H_2O$$

@ 25 deg. C (ΔH_{298} = -158.4 KJ/mole)
@ 300 deg. C (ΔH_{573} = -130.8 KJ/mole)

n- octane

$$CO + \frac{17}{8}\ H_2 \rightarrow \frac{1}{8}\ n\text{-}C_8H_{18} + H_2O$$

ΔH_{298} = -157.4 KJ/mole

toluene (typical aromatic product)

$$CO + \frac{11}{7}\ H_2 \rightarrow \frac{1}{7}\ C_7H_8 + H_2O$$

$$\Delta H_{298} = -138.5 \text{ KJ/mole}$$

methanol

$$CO + 2\ H_2 \rightarrow CH_3OH$$

$$\Delta H_{298} = -90.7 \text{ KJ/mole}$$

$$CO + 3H_2 \rightarrow CH_3OH + H_2O$$

$$\Delta H_{298} = -49.5 \text{ KJ/mole}$$

An example was worked through for steam reforming at 1000 K and syngas conversion at 500 K. Syngas composition leaving the reformer was assumed to be equal parts of carbon monoxide and dioxide to seven parts of hydrogen, as above. The syngas conversion catalyst was assumed to include water gas shift, Fischer-Tropsch, and shape selective functions. The TCPSA syngas conversion reactor will trap hydrogen over the syngas conversion catalyst while removing water from this zone, thus driving the shift conversion of CO_2 to CO.

It was assumed that the Fischer-Tropsch reaction is

$$CO + 2\ H_2 \rightarrow \frac{1}{n} C_nH_{2n}$$

$$(\Delta H_{298} = -153.2 \text{ KJ/mole})$$

The heat of reaction was estimated by assuming the product C_nH_{2n} to be 22.5% toluene and 77.5% n-octane. With the shift reaction included and a reaction temperature of 500 K, the heat of reaction in the syngas converter was estimated as

$$\frac{1}{2} CO + \frac{1}{2} CO_2 + \frac{5}{2} H_2 \rightarrow 1\ C_nH_{2n} + \frac{3}{2} H_2O$$

$$\Delta H_{298} = -112.3 \text{ KJ/mole}$$

Using the Stirling cycle data from Section 3.5, heat pumped to the reformer from the syngas converter is

$$-112.3 \times \frac{W1}{W2} = 112.3 \times \frac{33.94}{60.58} = 62.9 \text{ KJ/mole},$$

or 30.2 % of the 206.2 KJ/mole demanded by the steam reforming reaction. Hence, about 70% of the steam reforming heat must be provided by another source, in addition to thermal or mechanical energy required to make up energy dissipation losses within the TCPSA system. Some mechanical energy can be provided as compression energy of the feed.

The total mass balance is

$$CH_4 + \frac{3}{2} H_2O \rightarrow \frac{1}{2} CO + \frac{1}{2} CO_2 + \frac{7}{2} H_2$$

$$\rightarrow \frac{1}{n} C_nH_{2n} + \frac{3}{2} H_2O + H_2$$

with a net high grade heat requirement of

206.2 - 62.9 = 143.3 KJ/mole

delivered at 1000 K to the steam reformer. This heat may be provided by several alternatives, including:

- external heating by combustion of some of the surplus hydrogen from the syngas converter
- external heating by combustion of extra methane, leaving the surplus hydrogen as a valuable by-product
- internal heating by addition of oxygen to the reformer feed.

The latter alternative deserves closer examination. A ratio of 0.28 : 1 oxygen to methane will provide the necessary contribution to steam reforming heat. In effect, 56% of the methane is converted to syngas by partial oxidation , while the remaining 44% is converted by steam reforming. The overall reaction is mildly endothermic, in exact balance with the heat pumping capacity of the TCPSA reactor matched to syngas conversion. Heat exchange to an external furnace is eliminated.

A conventional methane partial oxidation reactor needs almost twice as much oxygen as the above oxygen-boosted TCPSA steam reformer. Despite high capital costs of tubular reformers, the cost of oxygen has previously discouraged application of POX processes to natural gas conversion. The above TCPSA process concept may be an acceptable hybrid approach.

Admission of oxygen to a TCPSA steam reformer (with low partial pressure of hydrogen) is expected to create problems with maintaining conventional nickel catalyst in a reduced state. Use of noble metal catalyst at the feed end of the catalyst bed may be necessary, as practised in POX methane to syngas conversion by BASF (reference S2, page 168).

It may be noted that some methane will leak through the reforming catalyst, and will then be concentrated by TCPSA toward the syngas conversion reactor. The syngas conversion catalyst (operating under a high partial pressure of hydrogen) is likely to produce a significant amount of methane, which will accumulate over the syngas conversion catalyst. This methane and excess hydrogen must be purged, at a rate which may be varied as a means of controlling the operation. The hydrogen may be separated as by-product and the methane recycled to the reformer, or the purge mixture may be used as a fuel.

Carbon deposition is unlikely to be a problem in TCPSA reactors because high steam and hydrogen partial pressures are maintained over the reforming and syngas conversion catalysts respectively.

High hydrogen partial pressure may push F-T reaction selectivity towards methane and higher saturated hydrocarbons, while high space velocity may encourage a kinetic selectivity toward olefins.

Stringent removal of sulphur from the methane feed is necessary, because the TCPSA steam reformer would tend to accumulate sulphur compounds with the trapped steam. Some purge of steam may be desirable to protect the catalyst.

3.8 Physical Size Estimates

Physical proportions of a TCPSA compound steam reforming / F-T reactor are estimated for a gasoline output of 50 bbl/day. This corresponds to 4.76 moles of methane converted per second. At a cycle rate of 10 RPM, 28.5 moles are converted per cycle. Steam reforming heat (W1) must then be 5.95 MJ per cycle. Hence the physical displacements used in the computer run of Section 3.5 must be scaled up by a factor of

$$\frac{5,950,000}{48.23} \equiv 123,000$$

or a linear scale of $(123,000)^{1/3} \simeq 50$. Hence, nominal piston diameter is

$$5 \text{ cm} \times 50 = 2.5 \text{ m}$$

With nominal piston strokes of 5 m, piston displacement is 24.54 m^3. Dead volumes are scaled from 150 cc to 18.45 m^3. This compares reasonably with an estimated steam reforming catalyst volume of 1.6 m^3 (with normal activity and effectiveness). The reactor's physical size could be reduced by operation at maximum pressures above the assumed 10 atmospheres.

Syngas production volume is 0.47 m^3 per cycle, with this volume referred to the nominal discharge pressure of 10 atm. The ratio of syngas production volume to expansion cylinder displacement is 0.47/24.54 = 0.019. This ratio is an important parameter for calculating the gas separation duty in delivering syngas from the cooler end of the reformer while trapping steam at the hot end, as discussed in Section 6 and Annex B below.

4.0 SELECTION OF ADSORBENTS

A literature survey was conducted into PSA and Stirling cycle technology, steam reforming and syngas conversion technology, and pertinent adsorbents. The bibliography and some discussion of key references are provided in Annex A of this report. No directly applicable published data was found referring to the physical adsorption of steam (or other gases) under the severe hydrothermal conditions of this application.

Considerable advice and assistance was obtained from D. Ruthven at UNB, R. Anderson at Union Carbide (Tarrytown, NY) and G. Keller at Union Carbide (South Charleston, W.Va.). Consensus opinion was obtained on the following points:

1. the general TCPSA concept seems valid, and has soundly based objectives as a new approach to managing reaction heat and equilibrium, but presents substantial developmental challenges;

2. application to high temperature steam reforming is an ambitious extrapolation of adsorption technology beyond previous industrial practice;

3. data on adsorbent performance prediction is not readily available. However, the common A and X zeolites will not survive in a severe hydrothermal regime, while silica dessicant is unlikely to provide required dynamic capacity at high temperature;

4. initially recommended candidate molecular sieves were silicalite and ultrastable Y zeolite, which have good stability despite limited dynamic capacity for water. An alumina adsorbent was subsequently recommended for experimental testing by Professor Ruthven.

Following the above advice, experimental samples were procured from Union Carbide of silicalite, ultrastable Y zeolite (cat cracking catalyst), and 13X zeolite for low temperature work. Reference W1 suggests that Union Carbide's new aluminum phosphate molecular sieves may also offer favourable stability and relatively hydrophilic behaviour. Dr. Ruthven also obtained samples of the recommended alumina adsorbent from Alcan.

Owing to the lack of available published data, an attempt was made to extrapolate available adsorbent isotherm data into the

regime of interest. This extrapolation was based on the well known linearity of adsorption isosteres over wide ranges of pressure and temperature conditions. For a given loading of the adsorbate (in this case, water), the isosteres are defined by

$$\ln\left[\frac{p_1}{p_2}\right] = -\frac{\Delta H}{R}\left[\frac{1}{T_1} - \frac{1}{T_2}\right]$$

The isosteric heat of adsorption H defines the slope of ln p versus 1/T.

Figure 7 shows the isosteres for water on 4A molecular sieve, extrapolating the published isosteres (reference R1, p.341) from normal working temperatures into the steam reforming range. This extrapolation is illustrative only, since 4A sieve lacks necessary hydrothermal stability. However, the projected dynamic capacity would be reasonable if the adsorbent could survive.

Figure 8 shows the extrapolated isosteres for silica gel, which has insufficient dynamic selectivity at high temperatures. The isosteres for normal conditions were obtained from reference K5.

Figure 9 shows isotherms for silicalite and 13X, at 24 deg.C, copied from reference R1, p. 18. The silicalite has low capacity at ambient temperatures. However, the isosteric heat of adsorption of water on silicalite is extremely low (about 6 Kcal/mole for low loadings), resulting in relatively flat isosteres as shown in Fig. 10. This extrapolation suggested that silicalite may be an acceptable adsorbent for the TCPSA steam reformer, as the dynamic capacity in the steam reforming range is projected to be about 0.5 mmole/g-at. However, this interpretation was subsequently invalidated by Dr. Ruthven's experimental results (see Figure 11), which showed that silicalite has greater selectivity for the carbon oxides than for water across a wide range of temperatures, and has insufficient capacity for water under the conditions of interest.

Available data on water adsorption over ordinary Y zeolite (Ca and Na cations) indicated reasonable sorption capacity for water, but no published data was found for water isotherms over the aluminum depleted ultrastable modification.It was expected that the ultrastable Y zeolite would be less hydrophobic than silicalite, and indeed this was confirmed by Dr. Ruthven's experimental results shown in Figure 13.

5.0 EXPERIMENTAL INVESTIGATIONS

5.1 Adsorbent Selectivity Experiments

A series of experiments were performed using a heated gas chromatograph column to obtain quantitative data on the selectivity of the chosen adsorbents to steam, the carbon oxides, and other constituents present during steam reforming of methane. These experiments were conducted by Dr. D.M. Ruthven's group at the University of New Brunswick.

The gas chromatograph column was heated at temperatures up to 400 degrees C, and operated at atmospheric pressures using helium carrier gas. Single component equilibrium coefficients were measured. These coefficients are the dimensionless ratios of concentration in the adsorbed phase to concentration in the gas phase, and were interpreted as the "Henry law" coefficients for the slope of the isotherms at low concentration. The equilibrium coefficients, K, are defined by equation 3 of Annex A. Heats of adsorption were estimated from the linear plots obtained of the equilibrium coefficients versus the inverse of absolute temperature. Latent heats were derived by the relation,

$$K = K_o e^{-(\Delta H/RT)}$$

which is valid for low adsorbent loadings (Ref R2).

Figure 11 shows the data obtained for Union Carbide silicalite. Water sorption is very low, indeed lower than either carbon monoxide or dioxide. Latent heat of adsorption for water is about 6.0 kcal/mole. It was concluded that a more polar aluminum containing adsorbent must be used.

Figure 12 shows data for a high area Alcan alumina adsorbent. Water sorption is projected to be high in the steam reforming temperature range, with a latent heat of about 10 kcal/mole. Carbon dioxide is also strongly adsorbed. Selectivity for water in favour of carbon dioxide will be small above 500 degrees C. Hence, a TCPSA steam reforming reactor using alumina will deliver syngas enriched in carbon monoxide (owing to the partial trapping of carbon dioxide in the reaction zone), which is desirable for synfuel production. Admixture of water gas shift catalyst in the adsorbent will enhance overall reaction rates.

Figure 13 shows preliminary data for a sample of ultra-stable Y zeolite obtained as powder from Union Carbide and pelleted at UNB for use in the chromatograph. Water is strongly adsorbed, similar to the alumina, but with a greater latent heat of 13.5 kcal/mole. Carbon dioxide is relatively less strongly sorbed at all temperatures. If both alumina and Y zeolite were otherwise equally qualified, the Y zeolite would be chosen for applications requiring hydrogen rich syngas (i.e. ammonia synthesis) while alumina would be preferred for methanol and F-T syntheses.

No hard data on hydrothermal stability of the above adsorbents was obtained, relative to the severe steam reforming regime. The amorphous alumina adsorbent may suffer a loss of area, which would be expected to affect capacity but not relative selectivity for the gases of interest.

5.2 TCPSA Apparatus

The experimental TCPSA apparatus was designed to perform PSA separations under an imposed temperature distribution and cyclic regime of pressure and flow corresponding to the proposed Stirling cycle reactor.

A schematic of Highquest's test rig is shown in Figure 14 and photographs of the apparatus appear in Figures 15 and 16. The test rig consists of two stainless steel cylinders referred to as the expansion cylinder and the compression cylinder. Located within each cylinder is a piston which is connected by a variable phase angle crank mechanism to a gearbox. The gearbox is driven by a 3/4 horsepower variable speed DC motor which permits test rig speeds of 0 to 60 rpm.

Attached to the end of the compression cylinder is a second stainless steel tube referred to as the displacer tube. Located within the displacer tube is a displacer. The displacer is attached to the displacer cylinder piston allowing the piston and the displacer to move as a single unit. The displacer was sized so that the volume of the displacer tube is filled by the displacer with minimum clearance.

An 11 inch long, 3/4 inch ID stainless steel adsorbent tube is attached to the end of the expansion cylinder. The adsorbent tube was packed with samples of various adsorbents during the course of the experiments.

Heating of the test rig was done through the use of a high temperature oven. The oven door was modified to allow the insertion of the displacer and adsorbent tubes into the oven. This arrangement permitted the heating of the test rig to temperatures of 1000 degrees C.

As shown in Figure 14, various valves and fittings are located on the test rig to facilitate the pressurization of the rig with the sample gas mixture as well as to provide a means of obtaining samples of the test rig contents. The sample valves were configured to permit independent sampling of the displacer and adsorbent tube contents. Water was introduced into the test rig by injection through a septum using a hypodermic needle. High pressure nitrogen was also introduced to the back side of the pistons to balance the pressures across the pistons and reduce the load on the motor. Pressure gauges were mounted on the displacer cylinder and the displacer tube to allow monitoring of the pressures within the test rig.

Analysis of the test rig contents was done using a Varian A-90 gas chromatograph having a thermal conductivity detector. Due to the difficulties associated with measuring water using a gas chromatograph, the chromatograph was configured in the two column arrangement shown in Figure 17. Column A was a 3 foot by 1/8 inch OD length of nickel tubing packed with 60/80 mesh Tenax. Column B consisted of 60/80 mesh Spherocarb packed in a 6 foot by 1/8 inch OD length of nickel tubing. The columns were connected by valve B in a manner that allowed column B to be disconnected from the flow path to the detector. Valve A was used to obtain a fixed volume sample in the sample loop and then introduce the sample into the chromatograph columns. With this two column arrangement, water could be separated in the Tenax column while the remaining light gases were separated in the Spherocarb column.

To avoid any possibility of condensation of water vapour in the sample lines or chromatograph columns, all components of the test rig containing water vapour that were not located in the oven were heated using heating tapes. The chromatograph columns and valves A and B were located inside the chromatograph's oven. All external sample lines and valves were also heated using heating tapes.

5.3 Procedure

To begin an experimental run, the test rig was first purged with a steady flow of nitrogen for several minutes. The nitrogen flow was then stopped and the rig was depressurized and sealed. Next, the rig was inserted into the oven and the oven was turned on. At the same time, the external heater tapes were turned on. Two to three hours were then allowed to elapse while the test rig was heated to the desired temperature. During the heat-up process, the chromatograph oven was brought to the desired temperature and the chromatograph was allowed to stabilize.

After the test rig had reached the desired temperature, a second purge with nitrogen was done. This was to ensure that no water from previous runs remained in the adsorbent.

Upon completion of the purge, the test rig was pressurized with the sample gas. A fixed volume of water was then injected into the test rig at the adsorbent tube. After injection of the water, samples were taken from the displacer and adsorbent tubes to establish the initial gas compositions.

Sampling and analysis of the test rig contents was done by opening the desired sample valve at the test rig. The sample valve at the chromatograph was then opened, trapping a sample in the sample loop. Switching sample valve A (Figure 17b) then introduced the sample into the chromatograph. For experimental runs using only nitrogen and water in the rig, column B was not used and the analysis was done using only the Tenax column. For runs in which nitrogen, carbon dioxide and water were used, the analysis procedure involved both columns. When the sample was first injected, both columns were switched on-line as shown in Figure 17c. After a predetermined time interval sufficient to allow the light gas components to pass through column A, column B was switched off-line (Figure 17b) thus trapping the light gases in column B. Analysis of the water was then done as before in column A. After the water had passed through the chromatograph, column B was again switched on-line and the analysis of the light gases was done.

Following the initial samples, the test rig motor was turned on and set to the desired speed. The rig was operated continuously over the duration of the experimental run. Samples were taken and the compositions of the displacer and adsorbent tube contents were determined at several intervals throughout the duration of the run. To insure the sampling method was consistent, all

samples were taken at top dead center of the compression stroke in the Stirling cycle (i.e. when the pressure was a maximum) and collected in a fixed volume sample loop. In addition, the samples were reduced to atmospheric pressure before they were introduced into the chromatograph. All samples were analyzed using the chromatograph immediately after they were taken.

After the completion of an experimental run, the test rig was depressurized and again purged with nitrogen. The oven and heating tapes were turned off and the rig was allowed to cool. Finally, the chromatograph columns were heated to 200 degrees C and helium carrier gas passed through them at a rate of 10 ml/min. The chromatograph was left this way over night to counteract any deactivation of the column packing that may have occurred during the experiments due to adsorption of water.

5.4 Results

Experimental runs were done to test a range of operating conditions. Runs were done for a temperature range of 400 to 800 degrees C. Partial pressures of water ranged from 1/2 to 2 atmospheres while total pressures were varied from 50 to 200 psig. Tests were done using both 13x and Alcan Aluminum alumina molecular sieves, though the majority of the tests were with the alumina. Both adsorbents were used in pellet form having a 1/16 inch diameter. All tests were performed with equal expansion and compression strokes and displacement volumes, and with the expansion crank leading the compression crank by a phase angle of 90 degrees.

The original intent of our experiments was to conduct the tests using a syngas mixture consisting of 10% carbon dioxide, 10% carbon monoxide, 10% methane and the balance hydrogen. Unfortunately, due to seal leakage problems resulting in potentially dangerous leaks into the oven, the experiments were conducted using nitrogen instead of the syngas mixture. Since it was anticipated that carbon dioxide would have the greatest effect on the process, some trials were also attempted using a mixture of nitrogen and carbon dioxide.

In total, 49 experimental runs were done, a detailed summary of which may be found in Annex C. Of the runs done, clear indications of separation of the water were obtained for 10 runs. Excerpts of the chromatographic analysis of several of these runs are given in Figures 18 to 21. These runs were done using the alumina adsorbent at temperatures of 400, 500, 600 and 800

degrees C. Additionally, these runs were done using a water partial pressure of 1 atmosphere (0.5 ml of water) and a total pressure of 100 psig of nitrogen. Finally, the runs were done operating the test rig as a Stirling cycle heat pump with a cycle rate of 10 rpm.

As can be seen from Figures 18 to 21, the water was clearly transported from the point of injection at the base of the adsorbent tube and concentrated in the displacer tube. These results are typical of all runs for which conclusive and repeatable results were obtained. Due to experimental limitations that will be discussed later, however, the results could not be repeated with enough accuracy to obtain quantitative results. Thus, all results obtained with the TCPSA test rig can only be considered qualitative in nature. This limitation of the results also made it impossible to determine the quantity of water that was transported between the adsorbent tube and the displacer tube.

During the course of the experiments, many problems were encountered that made it impossible to quantify the results. The most significant problems were those associated with doing the analysis of the water in the samples. Significant tailing of the water peaks made it very difficult to measure the water content of the samples. In many cases, deterioration of the Tenax column due to adsorption of water was detected resulting in a further reduction in the ability to accurately detect and measure the water.

Additional problems were caused by pressure leaks in the test rig and condensation of the water in areas that could not be heated. Leakage past the dynamic seals on the pistons resulted in a gradual loss of pressure in the test rig. This made it difficult to obtain repeatable samples over the duration of a run. In addition, the pressure drop meant the conditions in the test rig were changing during the run, further reducing the quality of the results. Condensation of the water obviously had a serious effect on the results and every effort was made to avoid this problem. Despite these efforts, however, small amounts of condensation was occasionally found on unheated surfaces such as the piston faces and inside the pressure gauges.

Effects of the operating conditions such as temperature, pressure and cycle rate could not be determined from the qualitative results of the batch separation runs. In general, there was far too much variation in the results from run to run to properly

assess the effects of these parameters. It was found, however, that separation of the water occurred more rapidly at the higher temperatures and that the separation was more complete. This probably reflects the kinetic limitations at low temperatures of using relatively coarse sized adsorbent pellets. Also, condensation of the water in the test rig did not occur at higher temperatures due to the higher overall temperature of the test rig. Thus, the apparent improvement of the separation at high temperatures could be due to improved detection of the water as a results of the elimination of condensation problems.

The effect of operating the test rig as a Stirling cycle motor was also tested. From Figure 20 it can be seen, as expected, that when the direction of rotation of the test rig was reversed (converting the Stirling cycle from "heat pump" to "engine" mode) the water was concentrated at the opposite end (the adsorbent end) of the test rig.

Finally, conclusive results could not be obtained with the 13X adsorbent. This is thought to be due to the lower temperatures used with the 13X to avoid damaging the sieve. Under these conditions, the 13X adsorbent would be irreversibly loaded and thus dynamically inactive at the working pressure of about 5 atmospheres.

As was previously mentioned, attempts were made to do several runs using a mixture of nitrogen and carbon dioxide in the test rig. Unfortunately, prior to doing these tests, significant damage was done to the test rig when it seized as a results of extended high temperature operation. The seizing of the test rig caused extensive damage to the inside of the displacer cylinder resulting in an inability to seal the piston and maintain the pressure in the rig. Thus, further results could not be obtained despite several attempts to do so.

To summarize the results, qualitative data were obtained that show water was separated on an alumina molecular sieve at elevated temperatures up to 800 °C. The results were obtained with enough repeatability to be certain of their validity. The separation was insensitive to the Stirling cycle mode (driving heat and steam together either to the hotter or the cooler end, i.e. operating in the "heat pump" or "engine" mode respectively).

6.0 ANALYSIS AND INTERPRETATION OF RESULTS

The quantitative data obtained at UNB for adsorbent selectivity over a wide temperature range was inserted into the theoretical models for the Stirling cycle and for equilibrium PSA cycles. The TCPSA steam reformer was analyzed according to the "normal Type I flow-controlled PSA cycle defined in Annex B. The following parameters were assumed:

pressure ratio	$\frac{P_2}{P_1}$	= 1.8
bed voidage	ε	= 0.35
effective equilibrium coefficient for water	K_A	= 5.0
effective equilibrium coefficient for syngas	K_B	= 0
steam concentration ratio in reaction zone (compression cylinder)	y_C	= 0.75
steam concentration ratio in syngas product (expansion cylinder)	y_E	= 0

This data was inserted into equation (41) of Annex C to establish the maximum theoretical productivity of dehydrated syngas, as a function of expansion cylinder displacement. It was thereby confirmed that the physical proportions of the methane steam reformer for the projected 50 bbl/day TCPSA methane to liquid fuel plant discussed in section 3.7 above are plausible, as the adsorbent volume and piston displacements seem comfortably capable of retaining the steam in the hot steam reforming reaction zone, while delivering dry syngas at rated productivity.

For the example discussed in Section 3.7,

$$\frac{\ell_{PROD}}{\ell_E} = 0.019$$

From equation (42) of Annex B , complete separation of a trace steam component from hot syngas should be achieved if

$$\frac{\ell_{PROD}}{\ell} < \frac{(B_B - B_A)}{B}\left[1 - \left[\frac{P_1}{P_2}\right]^B\right] = 0.514$$

using $B_A = 0.097$ and $B_B = 1.0$ derived from equation (4).

This simplified analysis suggests that syngas production rate might be increased over the actual rate by a factor of 0.514/0.019 = 27 before overwhelming the capacity of the TCPSA separation function to retain all the steam in the hot end. Of course, the analysis includes many approximations. A sufficiently rigorous computer simulation would incorporate the thermal gradient in the adsorbent bed, among many other important effects. The present preliminary analysis is thought to be conservative in using a relatively low value for corresponding to adsorbent selectivities expected toward the hot end of the adsorbent bed, i.e. at temperatures above 600 degrees C as shown by Figures 12 and 13. Adsorbent capacities will of course increase rapidly toward the cooler end of the bed, weighting the effective sorption capacity of the entire bed.

The above simplified analysis neglected carbon dioxide as a separate component. As discussed in Section 5.4, mechanical deficiencies prevented satisfactory tests of the TCPSA test rig with syngas containing carbon dioxide. The experimental data in Section 5.1 (using the heated chromatograph column at UNB) showed that both alumina and ultra-stable Y zeolite have satisfactory selectivity and capacity for steam relative to the light syngas components. However, alumina also adsorbs carbon dioxide almost as strongly as steam at high temperatures; so an alumina-based TCPSA reformer will trap carbon dioxide over the steam reforming catalyst to a considerable degree, so forcing the kinetic selectivity toward carbon monoxide formation as favoured for methanol or Fischer-Tropsch synthesis. This result is seen as favourable for natural gas conversion to liquid fuels.

The ultra-stable Y zeolite has lower selectivity for carbon dioxide, and thus would produce syngas with a carbon monoxide / carbon dioxide ratio close to that expected from steam reforming at the selected temperature and steam/carbon ratio.

7.0 CONCLUSIONS AND RECOMMENDED FUTURE WORK

All results obtained from the present project are positive, and are consistent with the prospective feasibility of TCPSA steam reforming reactors. Scientific feasibility of the process seems highly probable, although integration of the actual reaction with the TCPSA gas separation module has not been attempted yet.

Engineering and economic feasibility have not been demonstrated at this early stage. Major questions include adsorbent hydrothermal stability, catalyst productivity under unsteady conditions, methane carryover with the syngas product, overall energy efficiency, and compatibility for integration to other process modules such as a downstream F-T reactor.

It is considered that further basic development of the TCPSA concept should be conducted for other applications (with much more moderate working conditions) before proceeding to experimental development of an integrated TCPSA steam reformer. In the natural gas to liquid fuel conversion program, the proposed Phase 2 activity which seems most logical is to generate experimental data from integrated TCPSA micro-reactors applied to syngas conversion and the controlled partial oxidation process, and correlate the test data with simple theoretical models. This Phase 2 work will complement the present results in providing a first overview of the methane to liquid fuel conversion field, seen from the particular perspective of the TCPSA reactor development.

The results obtained from this work show that the TCPSA concept achieves gas separations at extreme high temperature, and have advanced our overall understanding of this technology at both theoretical and experimental levels. These results give encouraging indications that this concept may be of practical relevance to future synfuel technology, including realization of a commercial liquid fuel from natural gas industry.

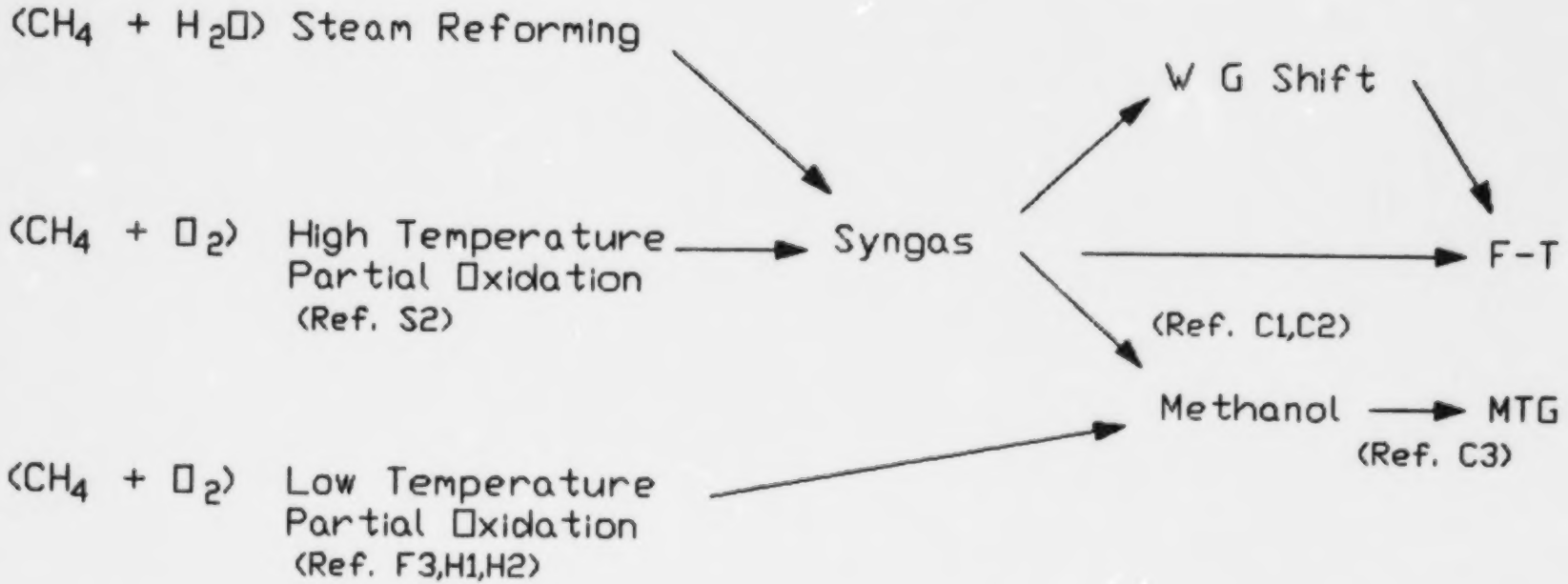

Figure 1: Methane to Gasoline Reaction Pathways

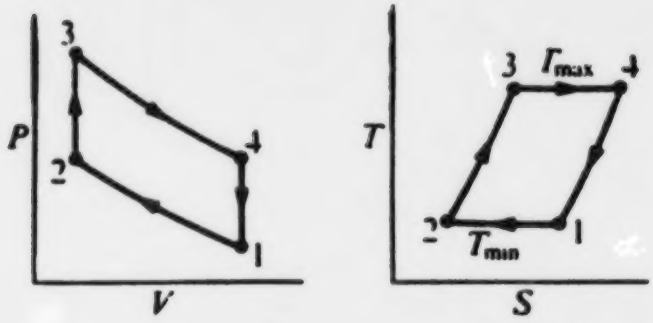

FIGURE 2a: P-V AND T-S DIAGRAMS FOR AN IDEAL STIRLING CYCLE

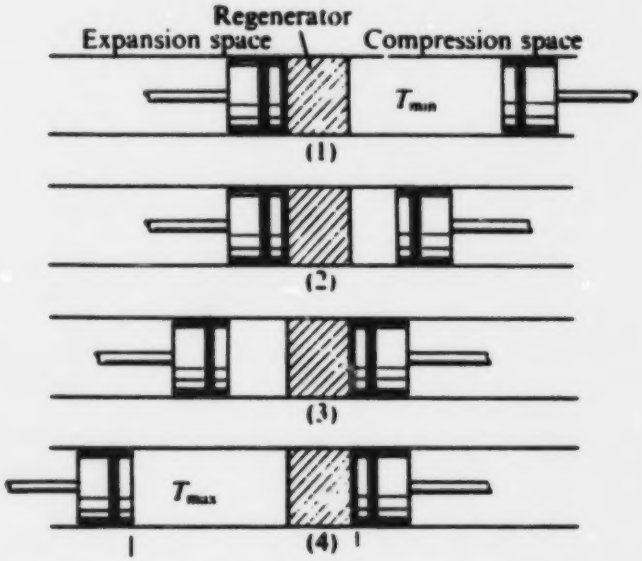

FIGURE 2b: TYPICAL PISTON MOTIONS FOR AN IDEAL STIRLING CYCLE

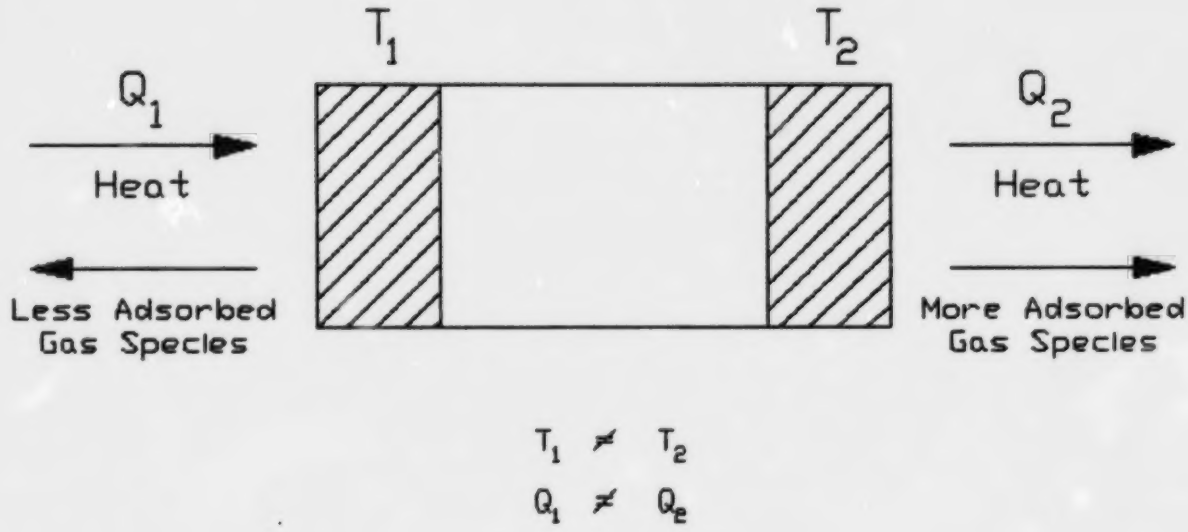

Figure 3. Directions of heat and mass transport in basic "TCPSA" module.

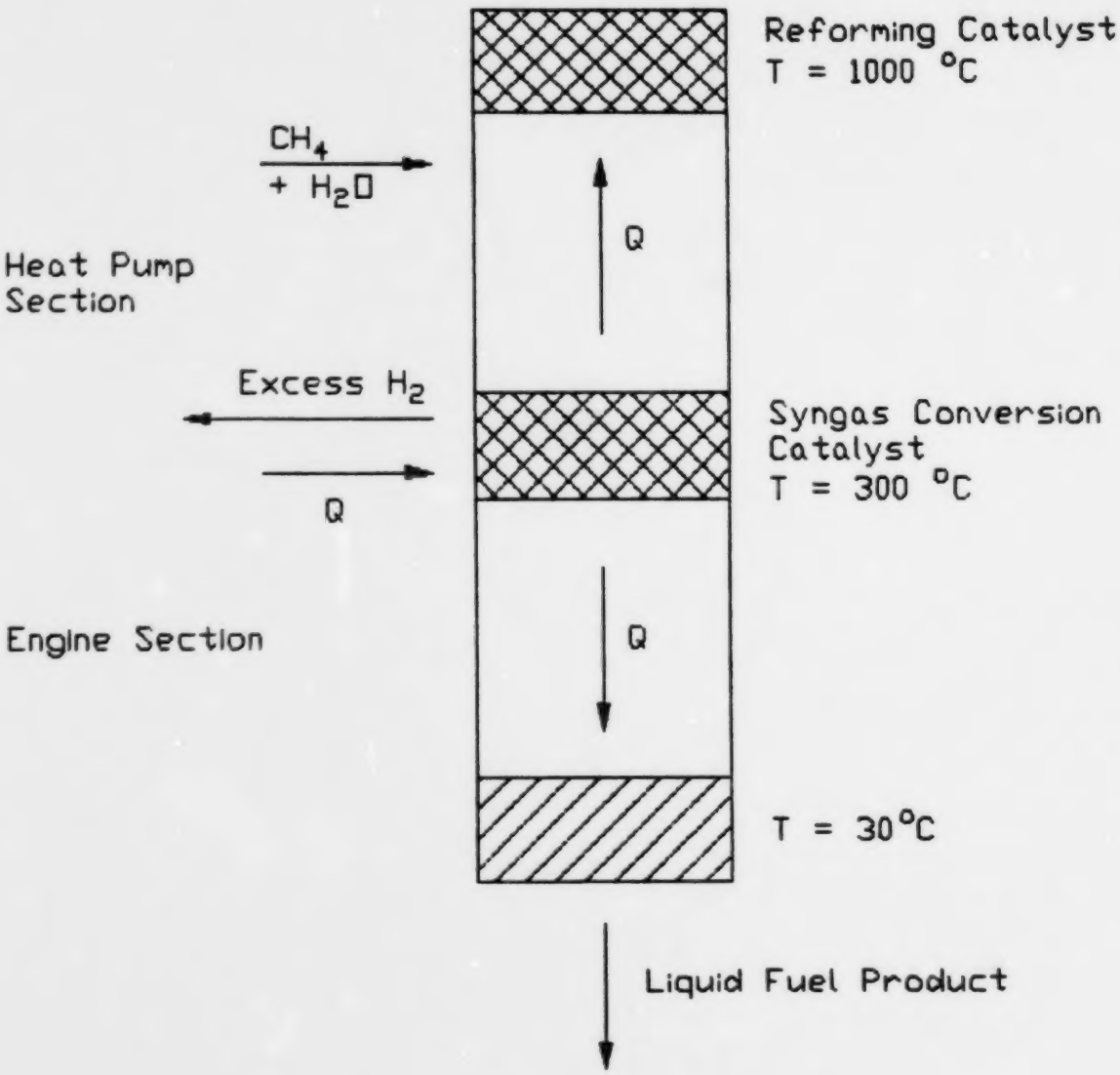

Figure 4. Schematic of a "TCPSA" Methane To Liquid Fuel Converter

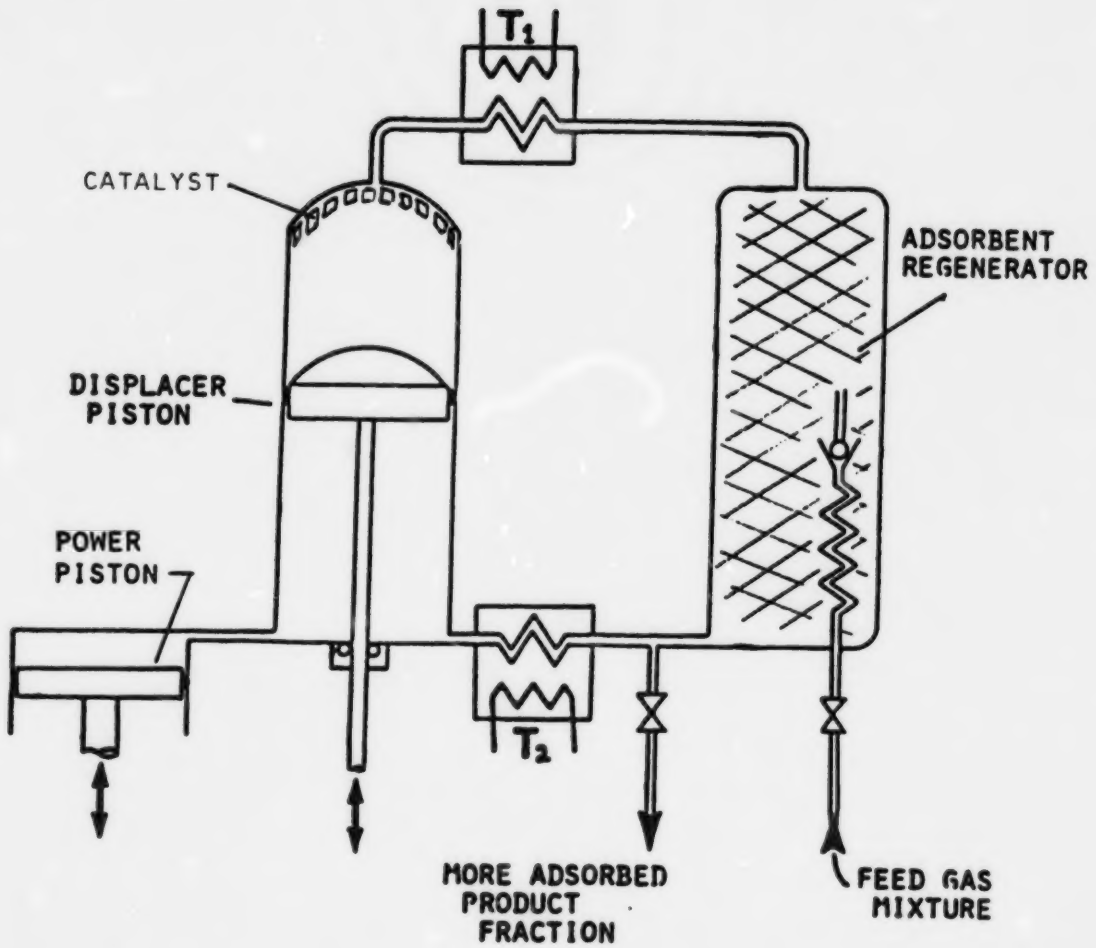

FIGURE 5: SCHEMATIC OF TCPSA REACTOR

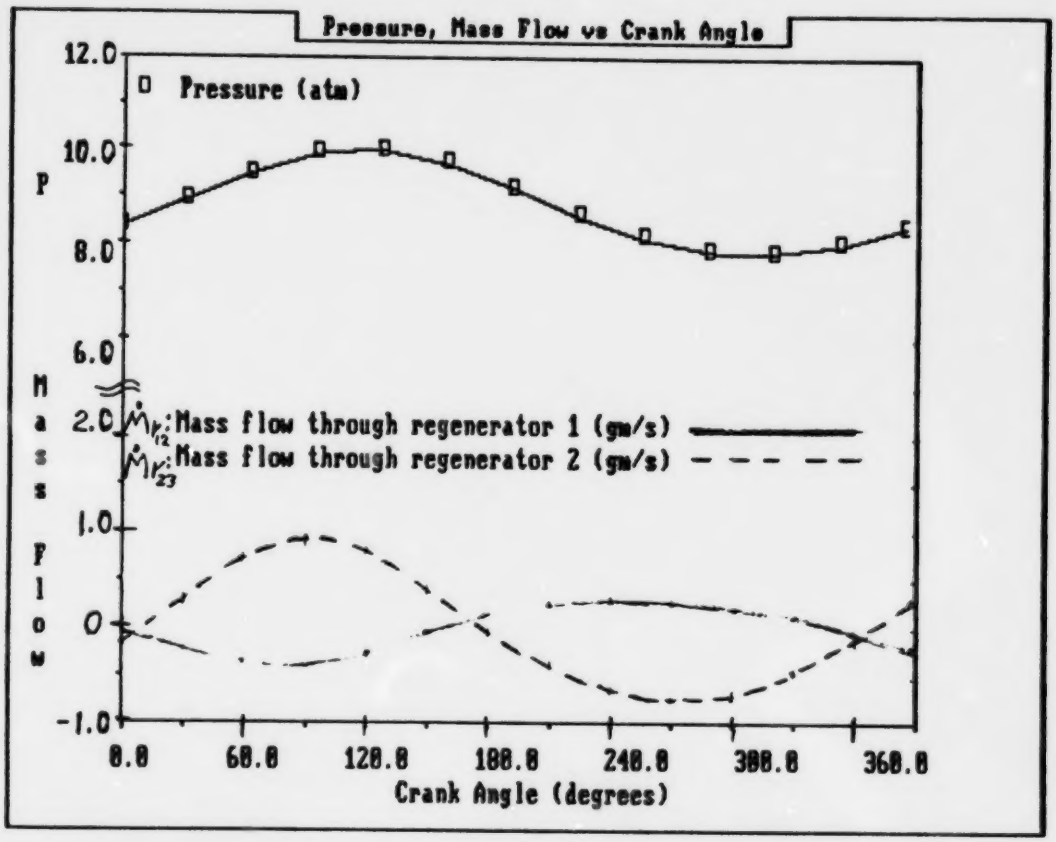

FIGURE 6: PRESSURE AND MASS FLOWS VS CRANK ANGLE FOR A TYPICAL MODELLING RUN OF THE COMPOUND STIRLING CYCLE TCPSA REACTOR

NOTE: REGENERATOR 1 IS IN TCPSA STEAM REFORMER.
REGENERATOR 2 IS IN TCPSA SYNGAS CONVERTER.

FIGURE 7

ISOSTERES OF H_2O ON 4A MOLECULAR SIEVE

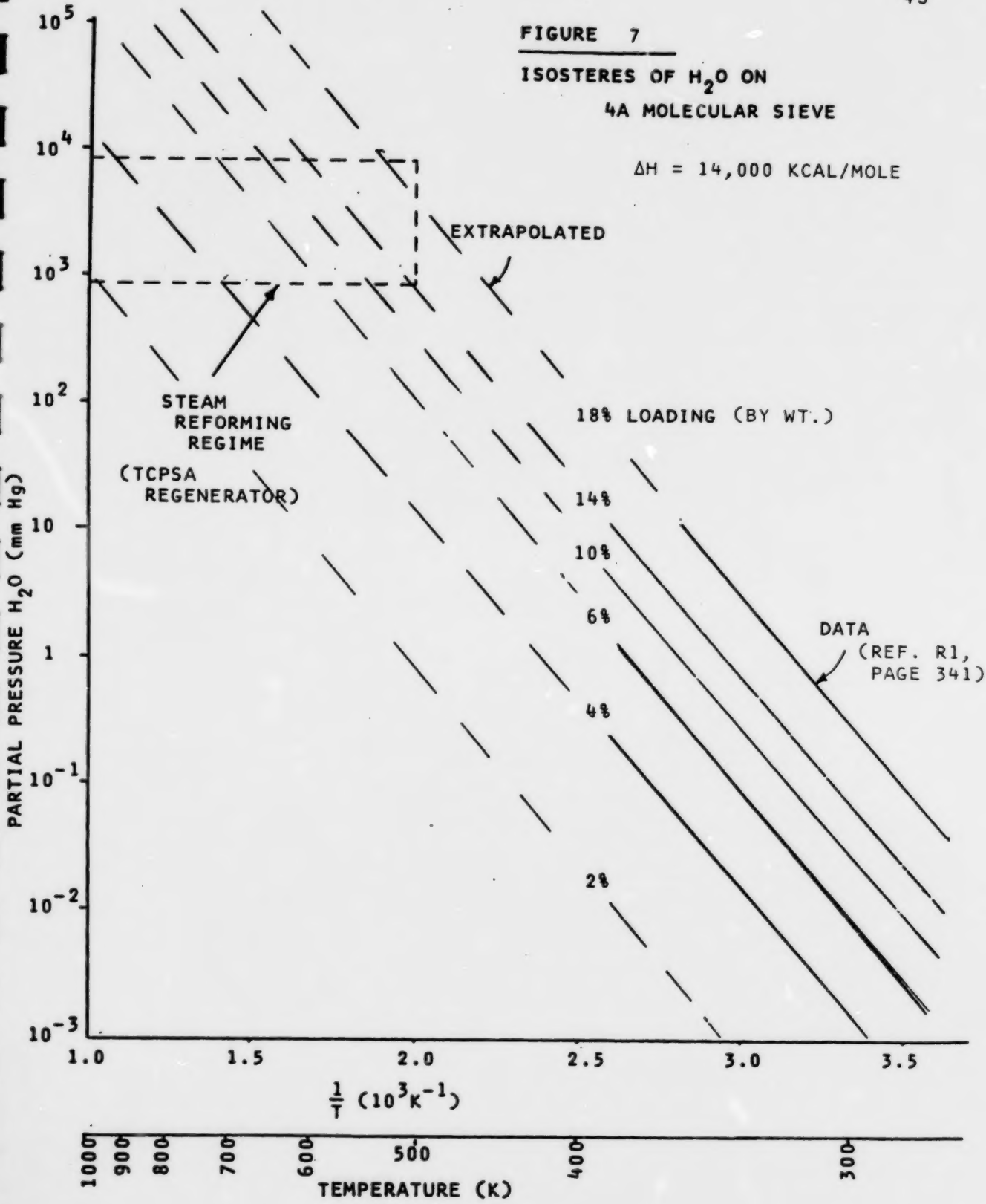

FIGURE 8

ISOSTERES OF H_2O ON SILICA GEL

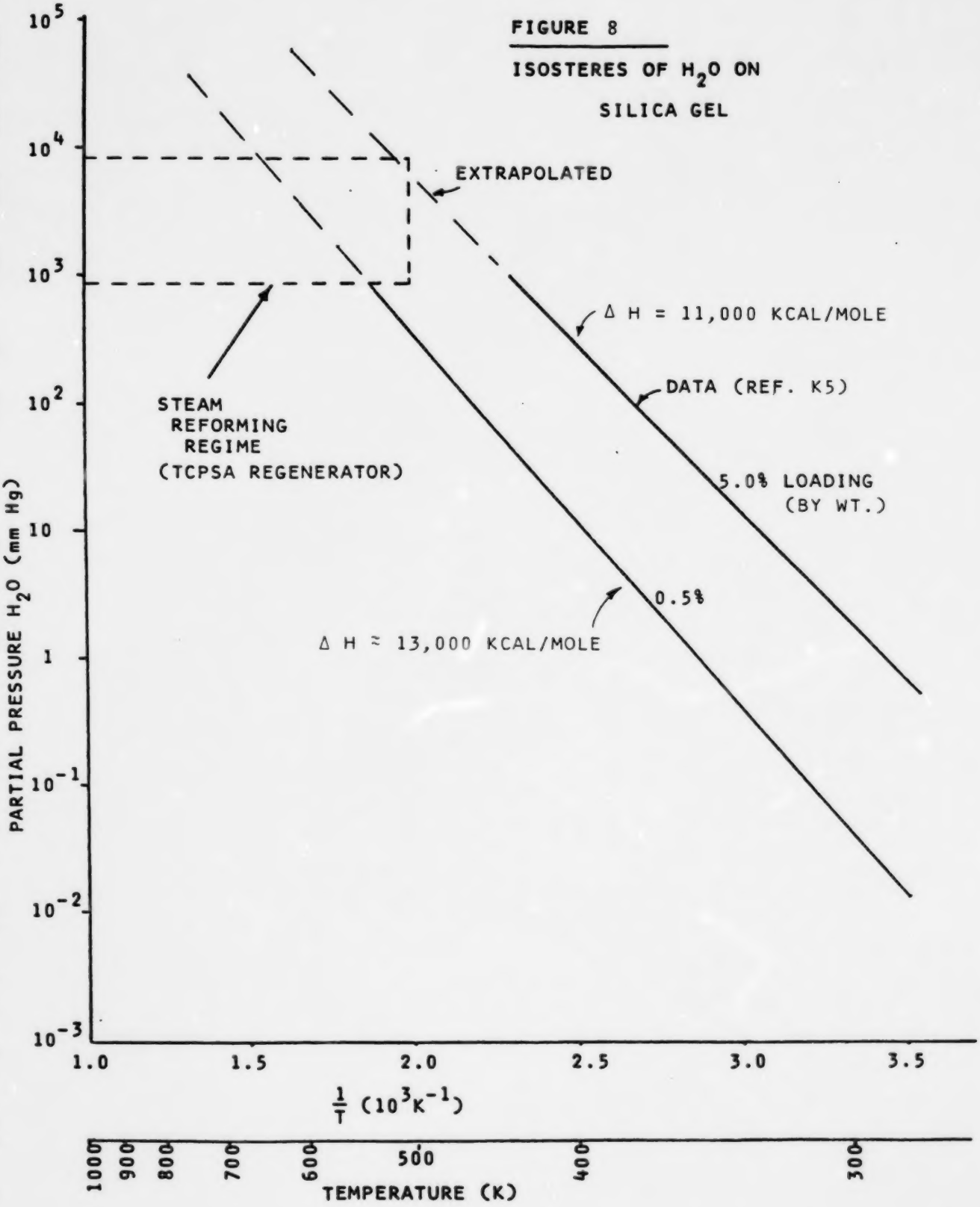

FIGURE 9

ISOTHERMS OF H_2O ON SILICALITE, NaX AND ALUMINOPHOSPHATE MOLECULAR SIEVES (REF. W1)

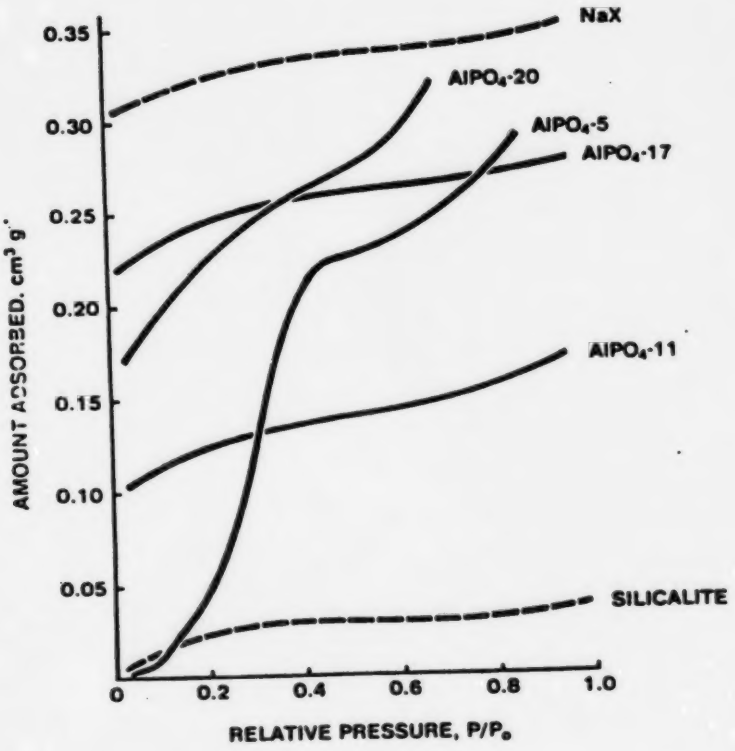

T = 24°C

P_0 = 22.4 mm Hg (SATURATION PRESSURE OF H_2O)

FIGURE 10

EXTRAPOLATED ISOSTERES OF H_2O ON SILICALITE

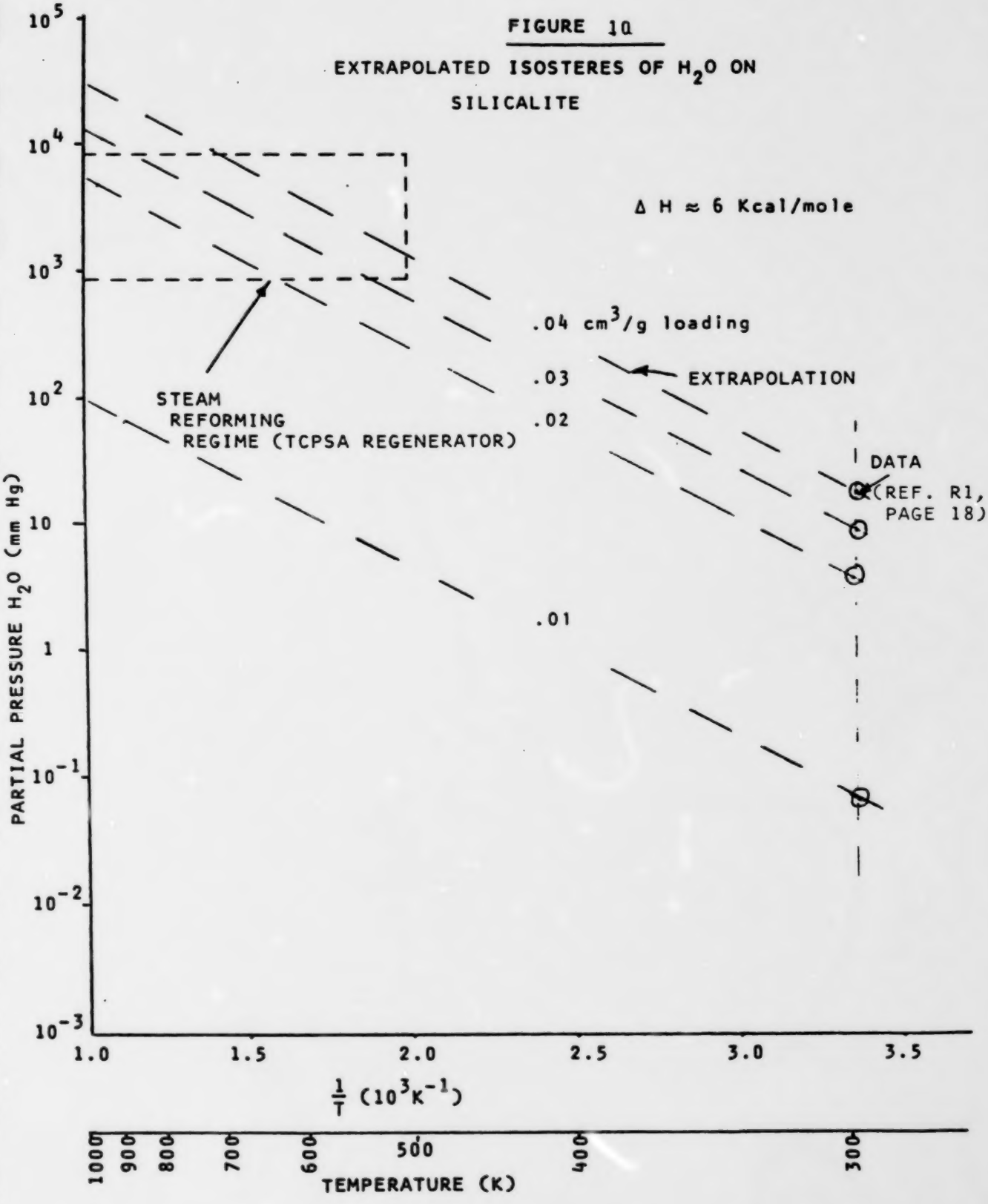

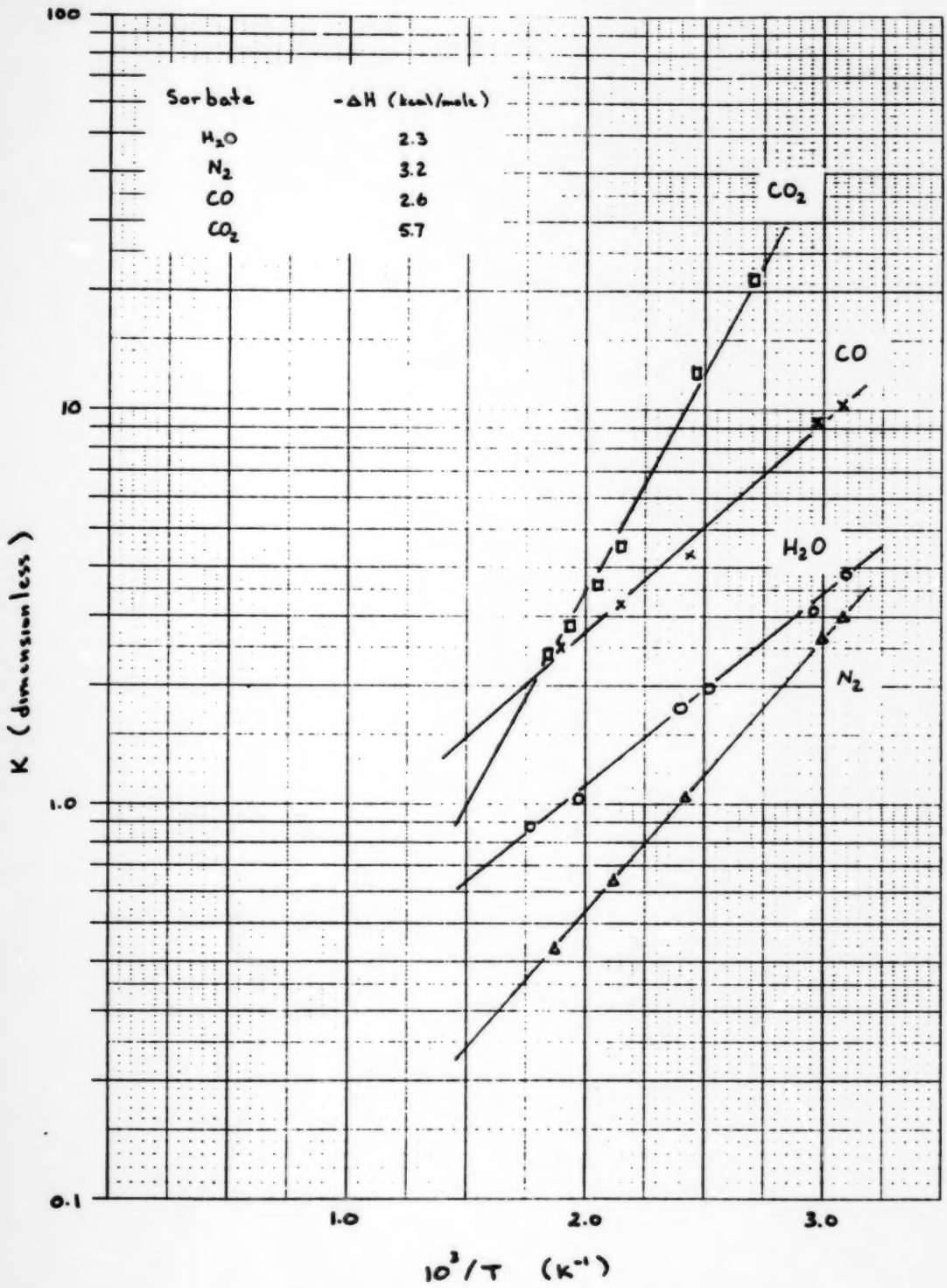

FIGURE 11: ADSORPTION EQUILIBRIUM COEFFICIENTS VS. TEMPERATURE FOR SILICALITE

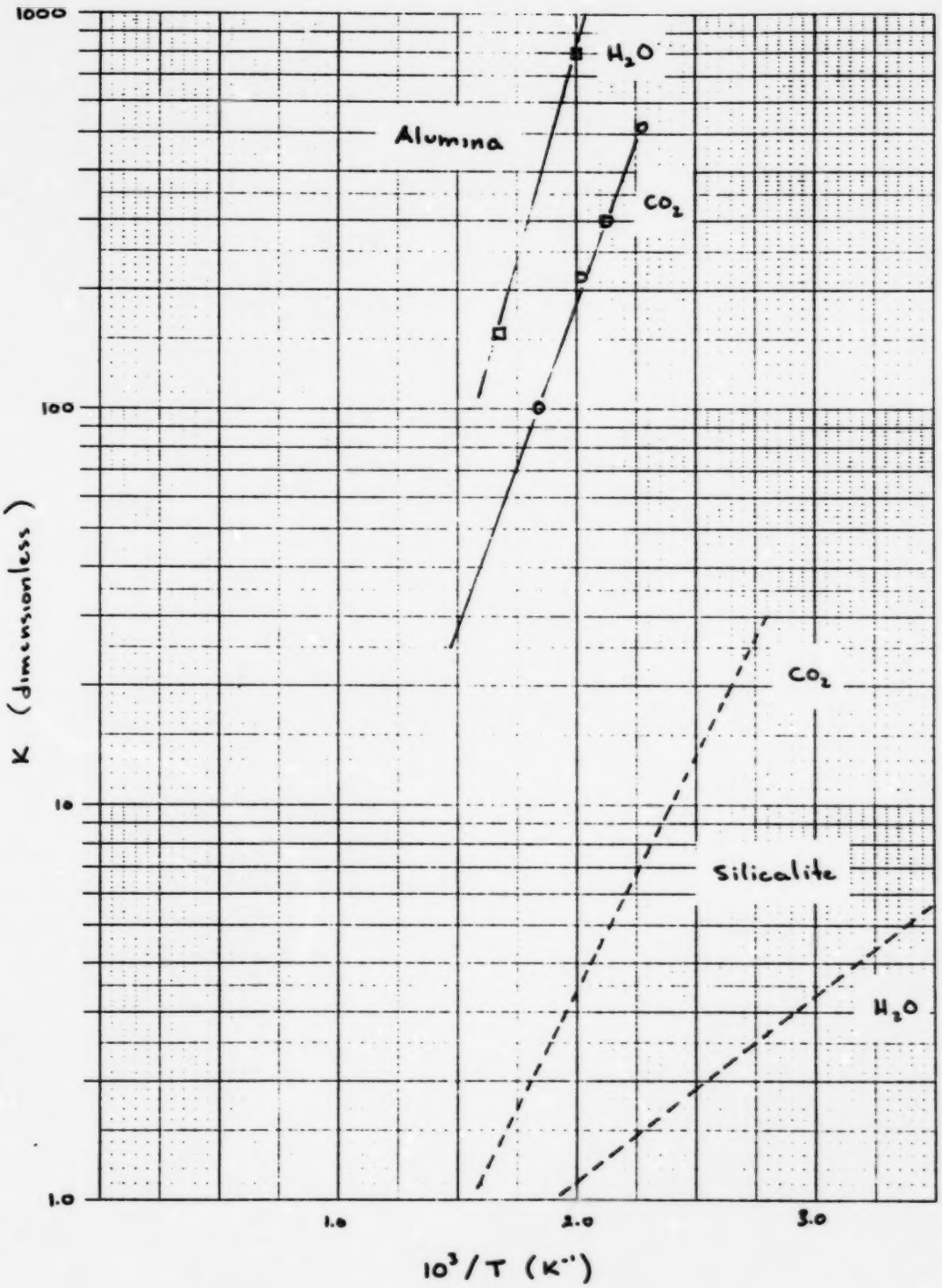

FIGURE 12: ADSORPTION EQUILIBRIUM COEFFICIENTS VS. TEMPERATURE FOR ALCAN ALUMINA

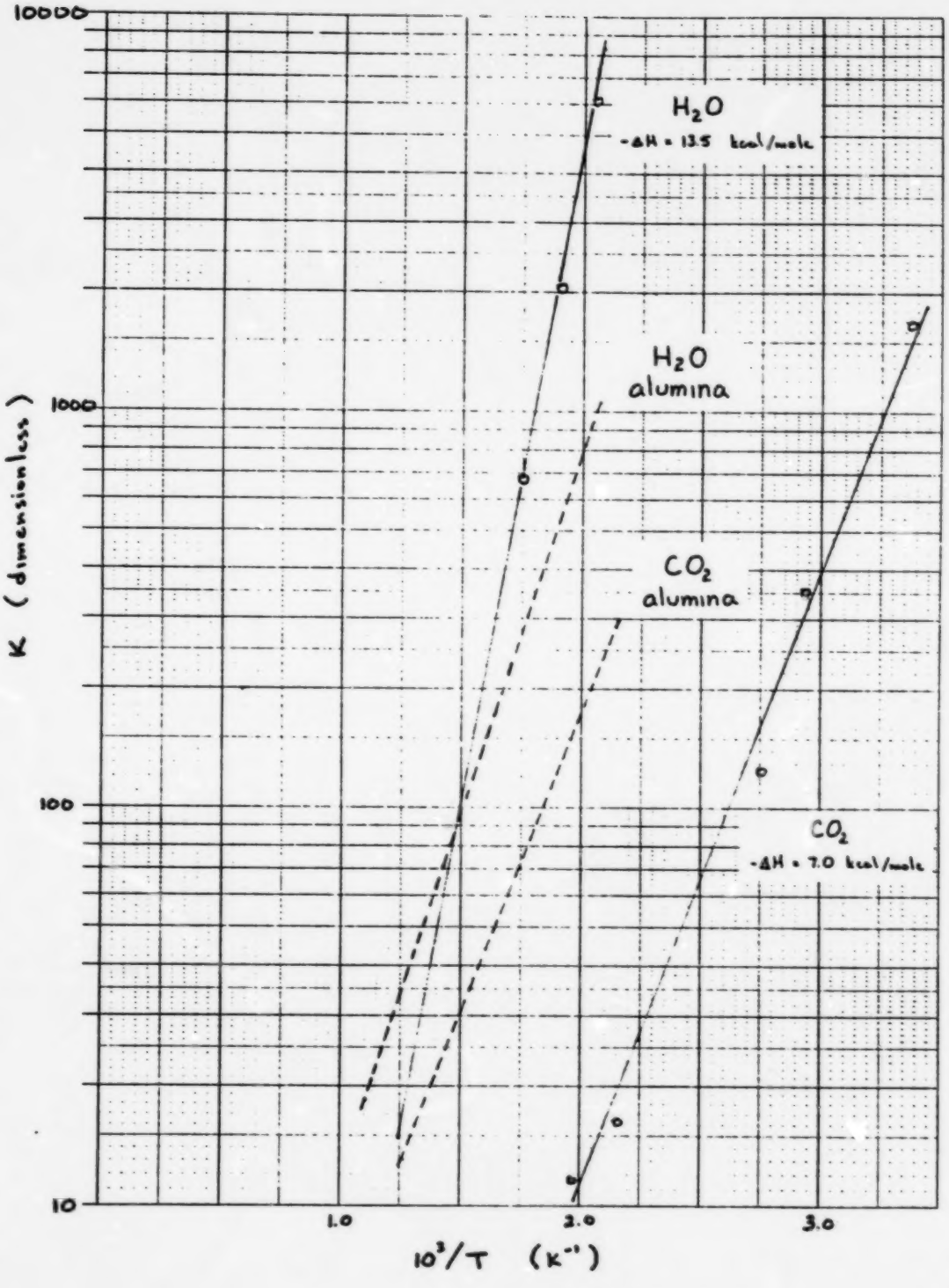

FIGURE 13: ADSORPTION EQUILIBRIUM COEFFICIENTS VS. TEMPERATURE FOR ULTRA STABLE Y ZEOLITE

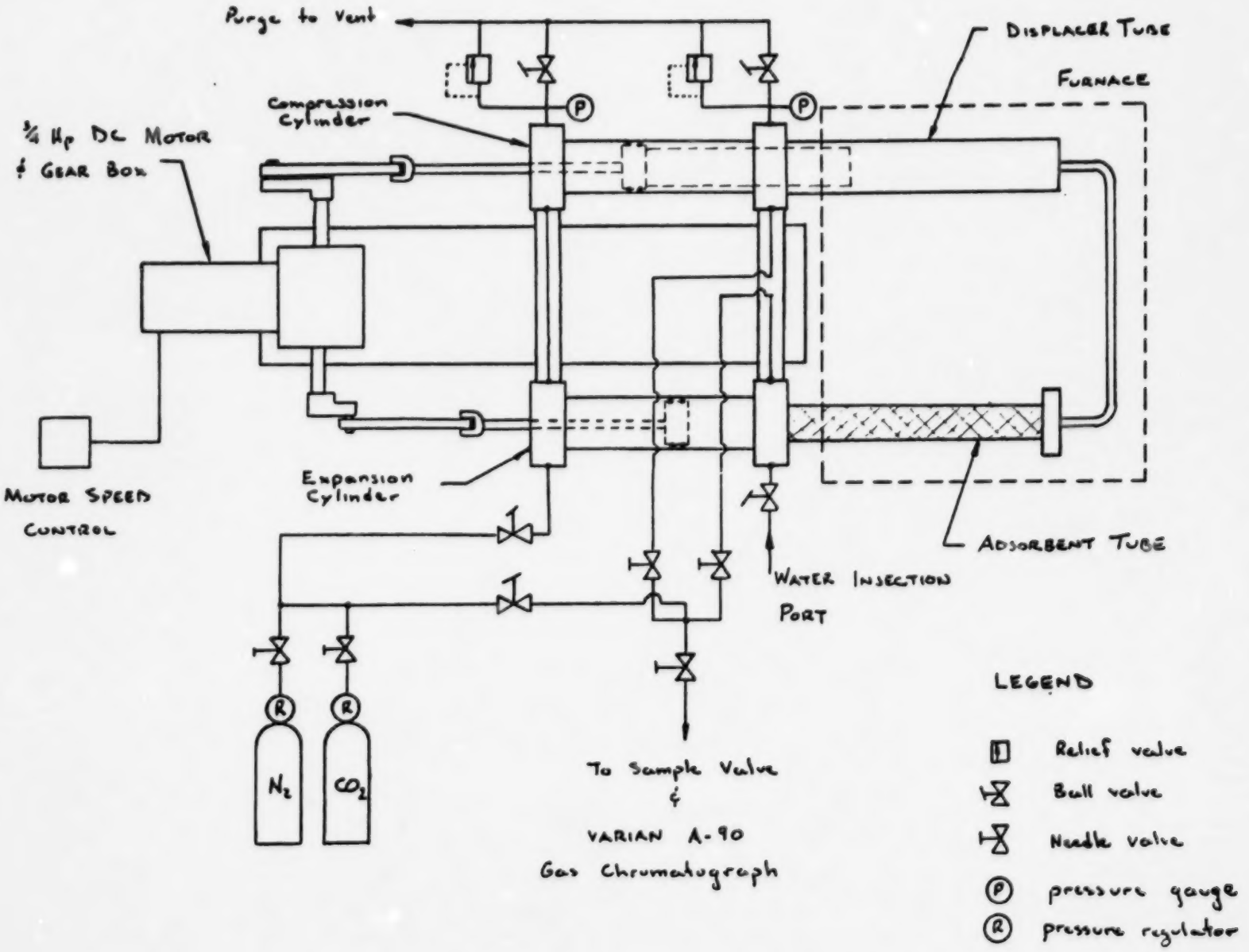

Figure 14: Schematic of the Highquest TCPSA test rig

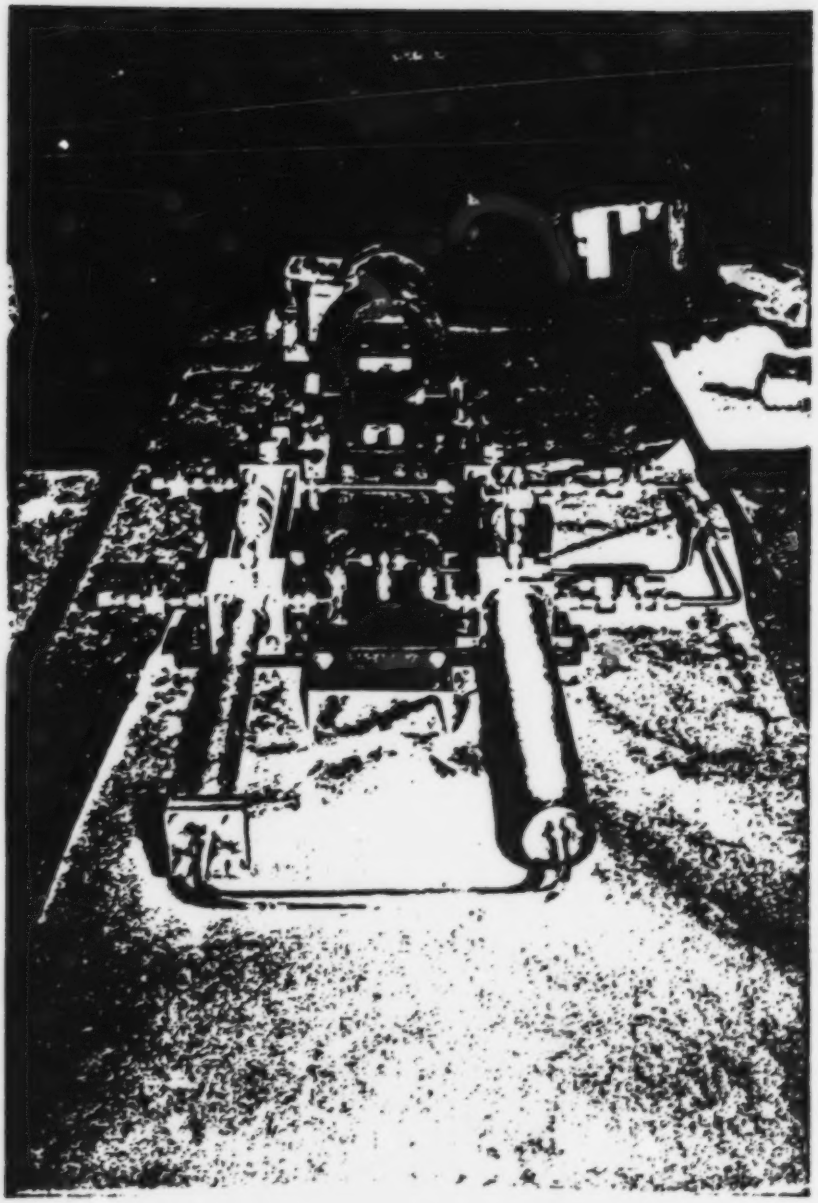

FIGURE 15: PHOTOGRAPH OF THE HIGHQUEST TCPSA TEST RIG

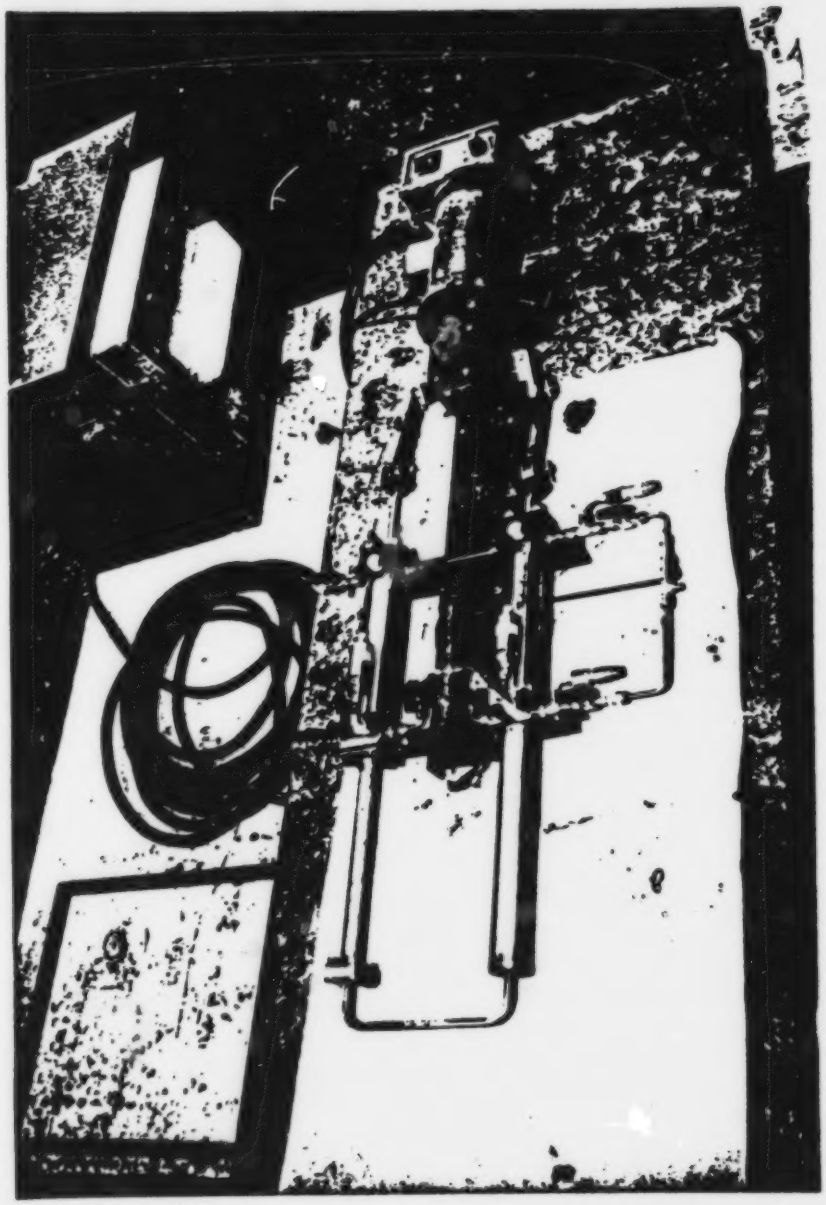

FIGURE 16: PHOTOGRAPH OF THE HIGHQUEST TCPSA TEST RIG

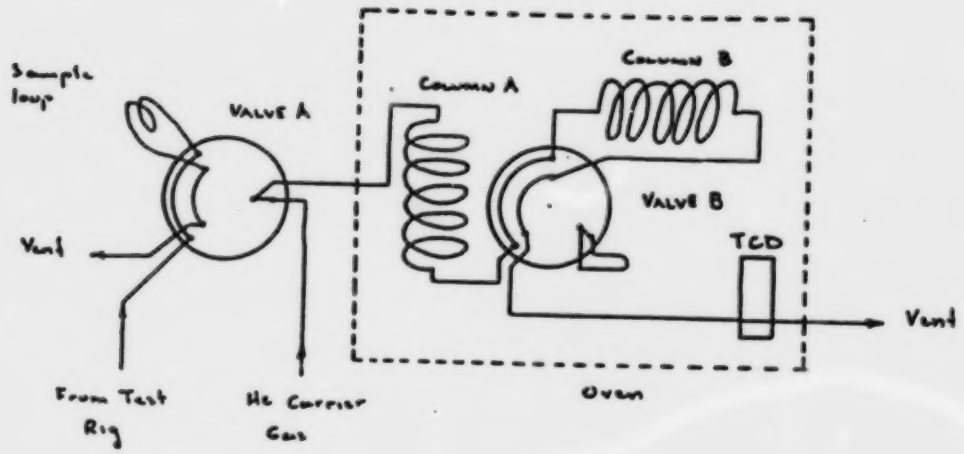

Figure 17a: Chromatograph configuration. Sample valve open and columns A and B in series with the TCD

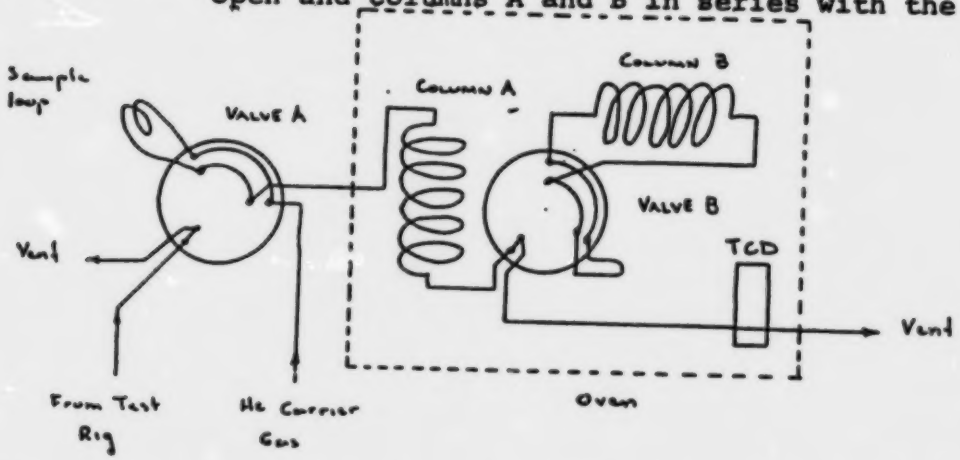

Figure 17b: Injection of the sample. Column A inline with the TCD, column B off-line

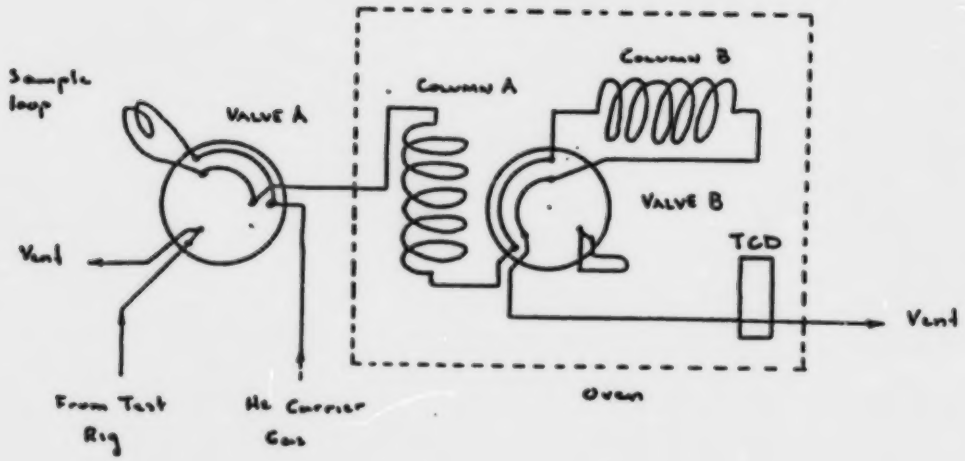

Figure 17c: Injection of the sample, columns A and B in series with the TCD.

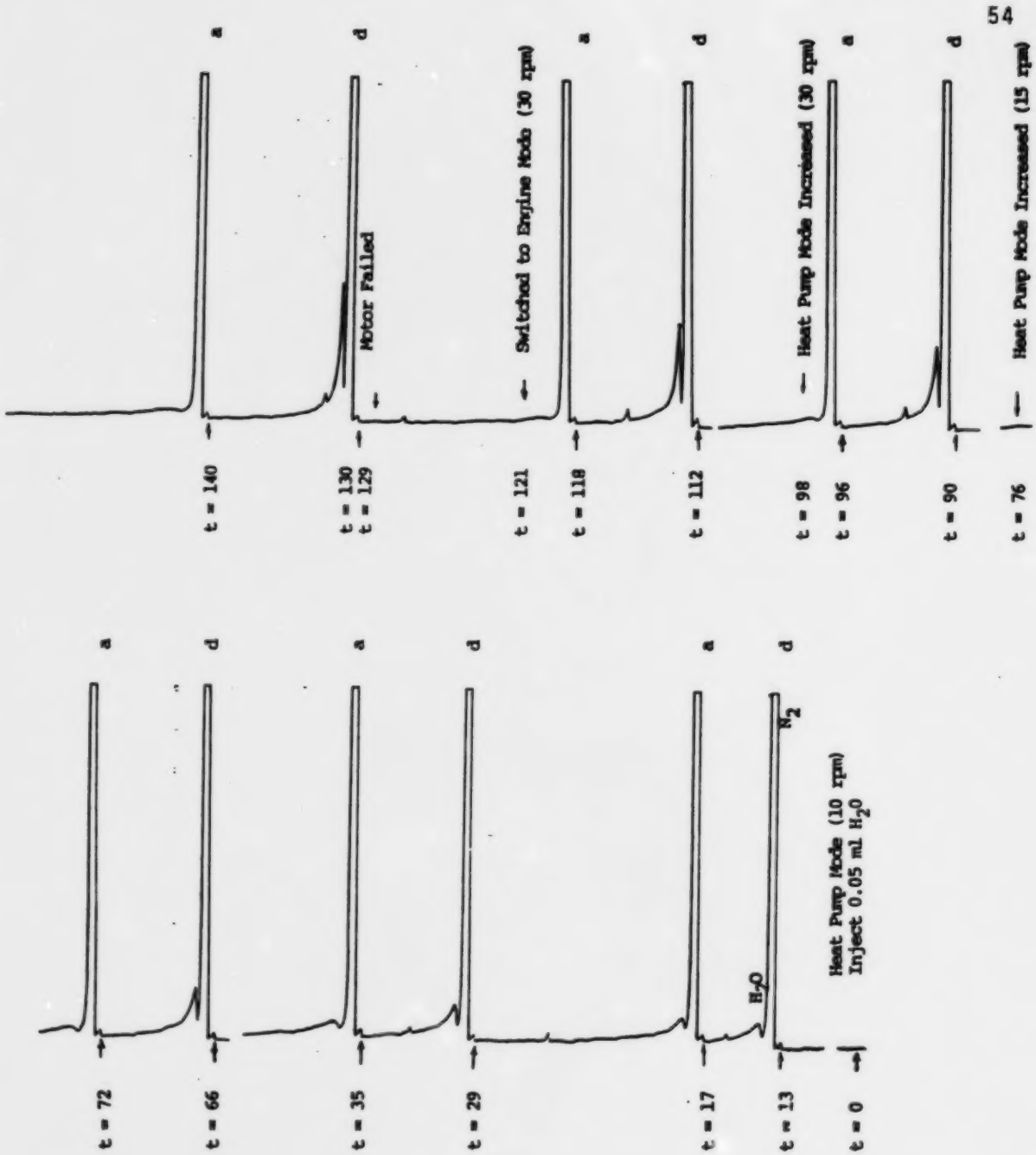

Chromatogram 040886-05

Conditions:
Column: 3 x 1/8 Tenax (Ni tube)
Column Temp.: 50 C
Attenuation 4
Carrier Gas: He

Key:
a = adsorbent end
d = displacer end
t = time (minutes)
→ = sample taken at time t

FIGURE 18: CHROMATOGRAM OF RUN # 040886-05
COMPONENTS - N_2, H_2O

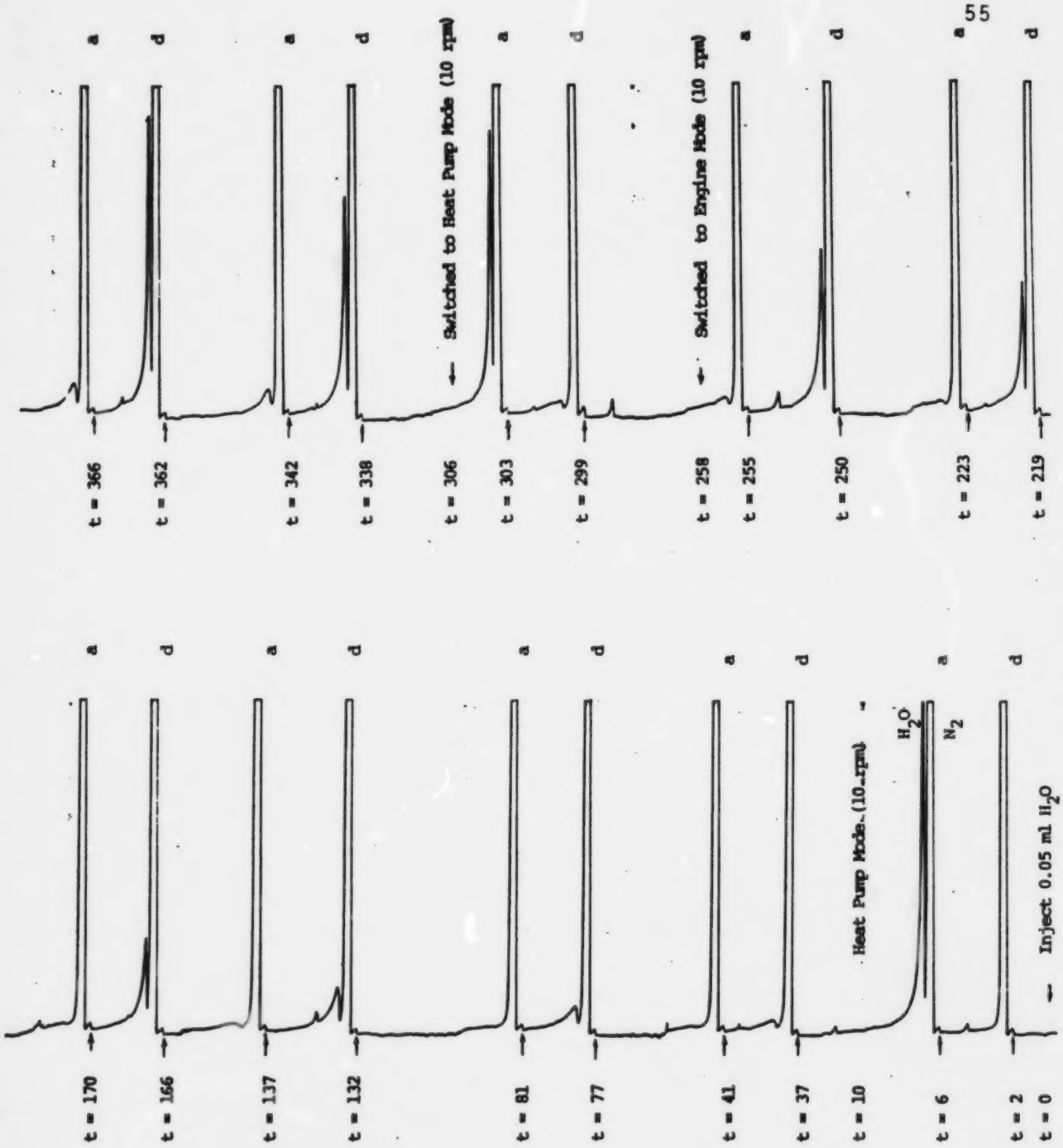

Chromatogram 041086-01

Conditions:
Column: 3 x 1/8 Tenax (Ni tube)
Colum Temp.: 50 C
Attenuation 4
Carrier Gas: He

Key:
a = adsorbent end
d = displacer end
t = time (minutes)
→ = sample taken at time t

FIGURE 19: CHROMATOGRAM OF RUN # 041086-01
COMPONENTS - N_2, H_2O

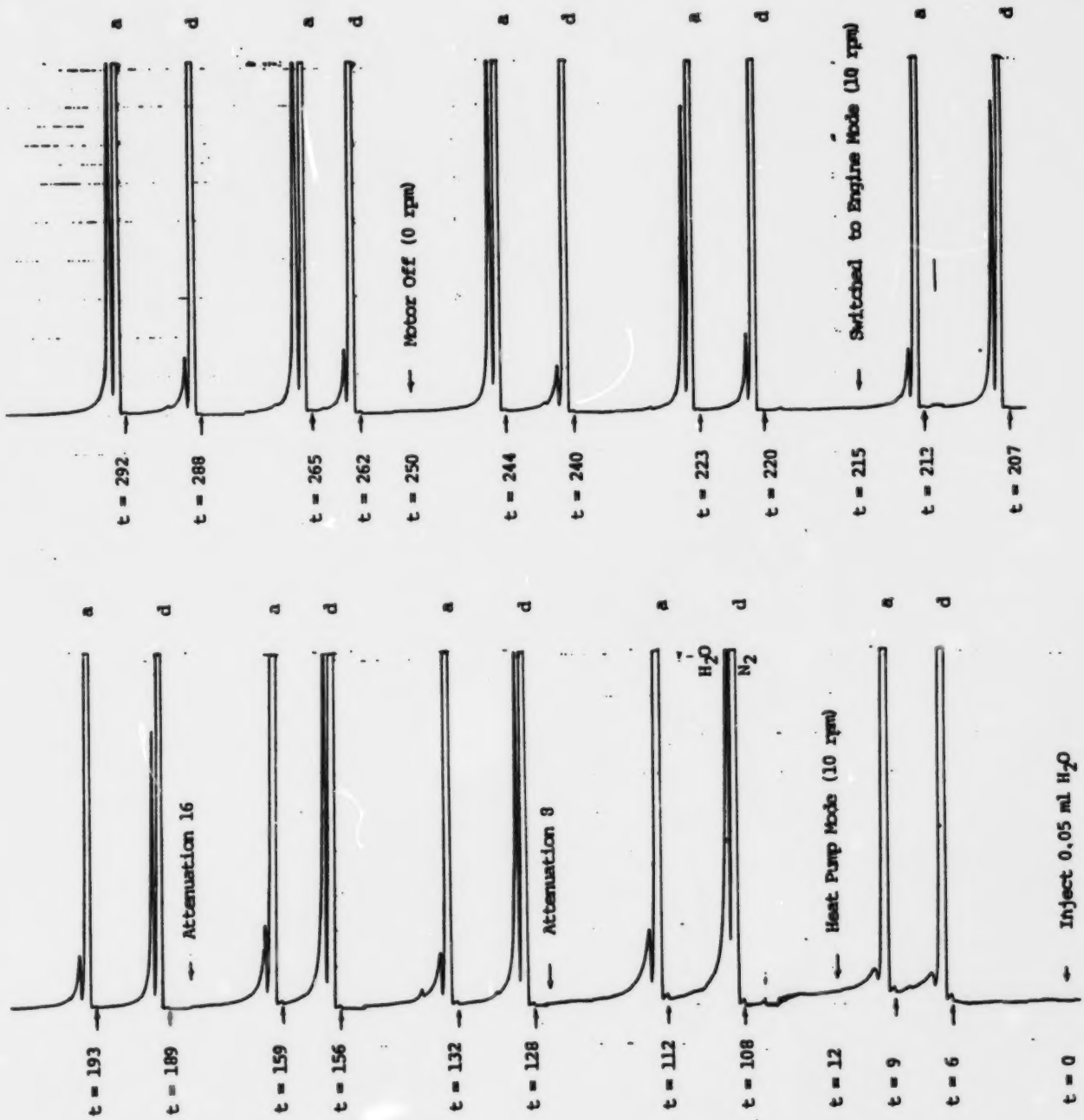

Chromatogram 041186-01

Conditions:
Column: 3 x 1/8 Tenax (Ni tube)
Column Temp.: 50 C
Attenuation 4
Carrier Gas: He

Key:
a = adsorbent end
d = displacer end
t = time (minutes)
→ = sample taken at time t

FIGURE 20: CHROMATOGRAM OF RUN # 041186-01
COMPONENTS - N_2, H_2O

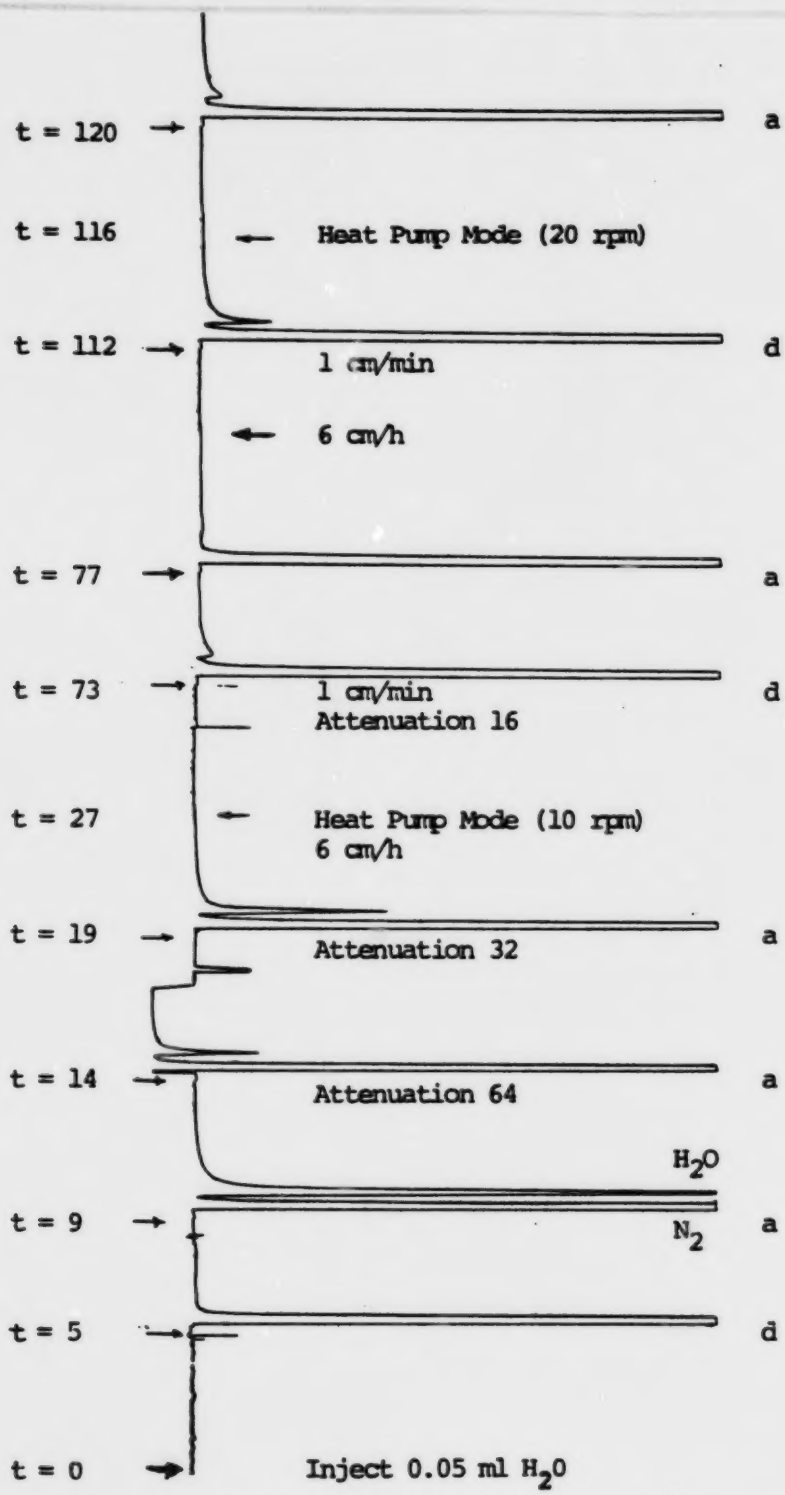

Chromatogram 041886-01

Conditions:

Column: 3 x 1/8 Tenax (Ni)
Column Temp.: 50 C
Attenuation 16
Carrier Gas: He

Key:

a = adsorbent end
d = displacer end
t = time (minutes)
= sample taken at time t

FIGURE 21: CHROMATOGRAM OF RUN # 041886-01
COMPONENTS - N_2, H_2O

ANNEX A

BIBLIOGRAPHY AND LITERATURE REVIEW

B1 G.W.Bridger, in
Catalyst Handbook
Wolfe Scientific Books, London, 1970

Review of steam reforming equilibria, catalyst selection and process engineering.

C1 C.D.Chang, W.H.Lang and A.J.Silvestri
Synthesis Gas Conversion to Aromatic Hydrocarbons
J.Cat. 56, 274, (1979)

Experiments on F-T synthesis using shape selective catalyst based on metal impregnated ZSM-5.

C2 P.D.Caesar, J.A.Brennan, W.E.Garwood and J.Ciric
Advances in Fischer-Tropsch Chemistry
J.Cat. 56, 274, (1979)

Experiments on F-T synthesis using mixture of iron and ZSM-5 particles to achieve shape selectivity.

C3 C.D.Chang
Hydrocarbons from Methanol
Catal.Rev.-Sci.Eng.25, 1, (1983)

Review of Mobil MTG process and related F-T synthesis using shape selective properties of ZSM-5.

D1 F.G.Dwyer and W.E.Garwood
Catalyst for Converting Synthesis Gas to High Octane predominantly Olefinic Naptha
U.S.Patents 4,361,503 and 4,463,101

Selectivity of ZSM-5 based F-T syntheses.

D2 J.C.De Deken, E.F.Devos and G.F.Froment
Steam Reforming of Natural Gas: Intrinsic Kinetics, Diffusional Influences, and Reactor Design
Chemical Reaction Engineering, ACS, (1982)

Useful but incompletely documented study of steam reforming kinetics and catalyst effectiveness.

F1 G. Flores Fernandez and L.N.Kenney
Modelling of the Pressure Swing Air Separation Process
Chem.Eng.Sci. 38, 827, (1983)

Equilibrium theory modelling of PSA, including effect of Langmuir isotherm curvature for one component.

F2 J.G.Finegold
Reformed Methanol Vehicle System Considerations
18th IECEC, 557, (1983)

Discussion of low temperature reactor for methanol cracking or steam reforming.

F3 N.R. Foster
Direct Catalytic Oxidation of Methane to Methanol- a Review
Preprint for Appl. Catal. (1985)

Review of technical and economic prospects of POX methane to methanol process compared to steam reforming.

G1 G. Gruber
Equilibrium Considerations in the Methane Synthesis System
Methanation of Synthesis Gas, 1974

Equilibrium analysis of coking tendency in methane steam reactions.

G2 H. Grober and S. Erk
Fundamentals of Heat Transfer, Third Edition
McGraw Hill, 1961

Includes mathematical analysis of cyclically forced heat transfer between gas and solid bodies.

H1 N.R.Hunter, H.D.Gesser, L.A.Morton and C.B.Prakash
The Direct Conversion of Methane to Methanol
Proc. VI Int.Symop. on Alcohol Fuels Technology, Ottawa, (1984)

Review and initial experimental results on POX of methane to methanol.

H2 N.R. Hunter, H.D.Gesser, L.A.Morton, and D.P.C. Fung
The Direct Conversion of Natural Gas to Methanol by the Controlled Oxidation at High Pressure

Preprint for 35th Canadian Chemical Engineering Conference, Calagary, 1986

Experimental results on POX of methane to methanol.

K1 G.E.Keller II and C-H.A.Kuo
Enhanced Gas Separation by Selective Adsorption
U.S.Patent 4,354,859 (1982)

Pioneering invention on operation of PSA column by out-of-phase pistons at each end, enabling independent control of pressure and flow to optimize adsorbent productivity and to obtain high recovery and purity of both light and heavy components.

K2 B.G.Keefer
Thermally Coupled Pressure Swing Process
U.S.Patent Application 06/538,370 (1983)

Discloses TCPSA principles, generalizing flow controlled PSA to include integration of PSA with Stirling cycle and also with chemical reactions.

K3 K.S.Knaebel and F.B.Hill
Pressure Swing Adsorption, Development of an Equilibrium Theory for Gas Separations
Chem.Eng.Sci. 40,2351,(1985)

Development of equilibrium theory for two component mixture with linear isotherms and without dispersion, applied to conventional PSA cycles. This theory is generalized in Annex A of this contract report to include dispersion correction terms, to include static axial temperature gradients, and to enable independent control of flow and pressure using pistons.

K4 F.L.Kester, A.J.Konopka, and E.H.Camara
On-Board Steam Reforming of Methanol to Fuel the Automotive Hydrogen Engine
IECEC '75 Record, 1975

Catalyst selection and reactor design for low temperature methanol steam reformer.

K5 A.L. Kohl and F.C. Riesenfeld
Gas Purification, third edition
Gulf Publishing Company, 1982

General review text, including a chapter on adsorption processes with emphasis on thermal swing dehydration.

L1 I.R.Leith
Hydrogenation and Fischer-Tropsch Synthesis on Zeolite Supported Group VIII Metal Catalysts
CSIR Report CEng 218, South Africa, 1977

Review of shape-selective catalysis and recommendations for further work.

L2 F.W.Leavitt
Non-Isothermal Adsorption in Large Fixed Beds
Chem. Eng. Progress, reprint supplied by Union Carbide.

Discussion of thermal effects in large PSA systems.

M1 R.Malpas, T.B.Anderson and J.M.Mitchell
"The Elegant Use of Oxygen", in
Oxygen and the Conversion of Future Feedstuffs
Proc. 3rd BOC Priestley Conference
Royal Society of Chemistry, London,(1983)

Lower cost oxygen would make POX competitive with steam reforming for conversion of methane to syngas.

P1 S.Paloumbis and E.E.Petersen
Coke Deposition on a Commercial Nickel Oxide Catalyst during the Steam Reforming of Methane
Chemical Reaction Engineering, 489, ACS, (1982)

Experiments on coking sensitivity to steam/carbon ratio.

R1 D.M.Ruthven
Principles of Adsorption and Adsorption Processes
Wiley-Interscience, 1984

Excellent comprehensive text on all aspects of adsorption technology.

R2 J.R.H.Ross and M.C.F.Steel
Mechanism of the Steam Reforming of Methane over a Co-Precipitated Nickel Alumina Catalyst
J.Chem.Soc. Faraday Trans. I69, 10, (1973)

Experiments on reaction kinetics at low pressures.

R3 J.R.Rostrup-Nielsen
Catalytic Steam Reforming, in
Catalysis, Science and Technology
ed. J.R.Anderson and M.Boudart
Springer-Verlag, 1984

Comprehensive report on steam reforming technology, including extensive review of prior work on catalyst properties, kinetics, coking, and interactions between nickel and alumina under hydrothermal conditions.

R4 D.M.Ruthven
Sorption of Oxygen, Nitrogen, Carbon Monoxide and Methane and Binary Mixtures of these Gases in 5A Molecular Sieve
A.I.Ch.E. Journal 22,753, (1976)

Experimental confirmation of theory for multicomponent adsorption.

S1 R.A.Sheldon
Chemicals from Synthesis Gas
D. Reidel, 1981

Includes reviews of steam reforming and recent approaches to F-T synthesis.

S2 S.Strelzoff
Ammonia Synthesis
Wiley Interscience, 1981

Good section on steam reforming and partial oxidation of methane to synthesis gas.

T1 D.Tondeur and P.C.Wankat
Gas Purification by Pressure Swing Adsorption
Sep. and Pur. Methods, 14(2), 157 (1985)

Excellent review of state-of-art PSA system engineering and comparison of alternative cycles.

U1 I.Urieli and D.M.Berchowitz
Stirling Cycle Engine Analysis
Adam Hilger, Bristol, 1984

Text on theoretical and numerical modelling of Stirling cycle machines.

W1 S.T.Wilson, B.M.Lok, C.A.Messina, T.R.Cannan and E.M.Flanigen
Aluminophosphate Molecular Sieves: A New Class of Microporous Crystalline Inorganic Solids, p.79 in Intrazeolite Chemistry, ACS, 1983

Water sorption on these adsorbents, with suggestion of high temperature stability.

ANNEX B

DEVELOPMENT OF EQUILIBRIUM THEORY FOR TCPSA SEPARATIONS

Introduction

Thermally Coupled Pressure Swing Adsorption (TCPSA) is a recently proposed (reference K2) class of pressure swing adsorption (PSA) gas separation technology, with the dual features of positive displacement control of flow direction and velocity, and a direct integration with the Stirling thermodynamic cycle. In TCPSA, separations are conducted over a single adsorbent column, which in general is subjected to a temperature gradient between its ends. An appropriate "parametric pumping" regime of optimally phased cyclic pressure oscillations and flow reversals is generated within the column by pistons (or equivalent displacement elements). The pistons are driven at the same frequency, with waveforms and phases selected to optimize both the selective transport of gas species by PSA, and the transport (and partial conversion) of heat by the Stirling cycle.

In the limit of zero temperature difference between the ends of the adsorbent column, the Stirling cycle is no longer invoked, and TCPSA degenerates into piston operated PSA systems of a class exemplified by the device invented by George Keller (reference K2). This class of PSA system is flow-regulated by the positive displacement pistons, in contrast to conventional PSA systems which are pressure-regulated by the opening and closing of valves connected to external pressure sources or sinks. The flow-regulated approach is fundamentally superior, in the following respects:

1) ideally, perfect recovery of expansion energy can be achieved, in contrast to the complete dissipation of expansion energy in simple conventional PSA systems and the substantial loss of expansion energy in more complex multi-bed conventional systems.

2) its considerable flexibility to achieve independent control of flow and pressure waveforms enables the flow-regulated PSA system to maximize productivity of the adsorbent, and to achieve essentially complete separation of a two component mixture into pure heavy and light components at opposite ends of the column. Conventional PSA can produce a pure light component fraction (with incomplete recovery), but is inherently incapable of producing a pure heavy component fraction.

3) in the presence of a thermal gradient between the ends of the column, the flow-regulated PSA cycle becomes TCPSA, and transports heat according to the Stirling cycle.

4) the flow-regulated PSA cycle can be directly coupled to chemical reactions, managing both the equilibrium (by PSA separation of desired products and reactants) and the heat of reaction (by the Stirling cycle).

Notation

C_i	concentration of component"i" in the gas phase $(mmole/cm^3)$
D_L	axial dispersion coefficient (cm^2/s)
K_i	equilibrium coefficient $K_i \equiv \frac{q_i}{C_i}$ (-)
ℓ_C	stroke of compression piston, normalized to column voidage area. (cm)
ℓ_E	stroke of expansion piston, normalized to column voidage area. (cm)
ℓ_{PROD}	product delivery, normalized to column voidage area (cm)
P	pressure (atm)
q_i	concentration of component "i" in the adsorbed phase $(mmole/cm^3)$
t	time (s)
T	absolute temperature (^0K)
u	flow velocity (cm/s)
y	gas phase concentration ratio $y \equiv \frac{C_A}{C_A + C_B}$ (-)
Z	axial distance (cm)
B_i	fraction of component "i" in the gas phase, defined by equation (4). (-)
B	ratio defined by equation (9). $B \equiv \frac{B_A}{B_B}$ (-)
ε	adsorbent bed voidage ratio. (-)

Subscripts

A	preferentially adsorbed (heavy) component
B	less adsorbed (light) component
C	compression piston
E	expansion piston
P	general piston
0	end of column

Equilibrium Theory

For a two component gas mixture flowing with longitudinal dispersion in an adsorbent column, continuity equations for the non-reacting components are

$$\varepsilon \left\{ \frac{\partial C_A}{\partial t} + \frac{\partial}{\partial Z} (uC_A) \right\} + (1-\varepsilon) \frac{\partial q_A}{\partial t} - \varepsilon D_L \frac{\partial^2 C_A}{\partial Z^2} = 0 \qquad (1)$$

$$\varepsilon \left\{ \frac{\partial C_B}{\partial t} + \frac{\partial}{\partial Z} (uC_B) \right\} + (1-\varepsilon) \frac{\partial q_B}{\partial t} - \varepsilon D_L \frac{\partial^2 C_B}{\partial Z^2} = 0 \qquad (2)$$

Assuming isothermal conditions, adsorption equilibrium with a linear isotherm, and the ideal gas law, the adsorbent loading relations are

$$q_A = K_A C_A = K_A \frac{yP}{RT}$$

$$q_B = K_B C_B = K_B (1-y) \frac{P}{RT} \qquad (3)$$

More general and valid adsorbent loading relations such as the Langmuir isotherm or multicomponent isotherms (see reference R1) may be substituted for equations (3). The temperature dependence of the isotherms must be incorporated for TCPSA systems with a thermal gradient imposed along the bed.

The column distribution coefficient B_i for a component "i" is defined as the fraction of that component in the adsorbent bed which is in the non-adsorbed gas phase. As will be seen from equation (17), the column distribution components determine the retardation of concentration wavefront velocity relative to bulk flow velocity. The column distribution coefficients are

$$B_i \equiv \frac{\varepsilon}{\varepsilon + (1-\varepsilon) K_i} \qquad (4)$$

With the assumptions that pressure varies only with time, and that temperature is constant in time and space, equation (1) becomes

$$\frac{1}{B_A P}\frac{\partial(yP)}{\partial t} + \frac{\partial(uy)}{\partial Z} - D_L \frac{\partial^2 y}{\partial Z^2} = 0 \qquad (5)$$

expanding to

$$\frac{1}{B_A}\frac{\partial y}{\partial t} + u\frac{\partial y}{\partial Z} + y\frac{\partial u}{\partial Z} + \frac{y}{B_A}\frac{\partial \ell n P}{\partial t} - D_L \frac{\partial^2 y}{\partial Z^2} = 0 \qquad (6)$$

Similarly, equation (2) becomes

$$-\frac{1}{B_B}\frac{\partial y}{\partial t} - u\frac{\partial y}{\partial Z} + (1-y)\frac{\partial u}{\partial Z} + \frac{(1-y)}{B_B}\frac{\partial \ell n P}{\partial t} + D_L \frac{\partial^2 y}{\partial Z^2} = 0 \qquad (7)$$

Equations (6) and (7) may be combined by direct addition to eliminate the dispersion term:

$$\left(\frac{1}{B_A} - \frac{1}{B_B}\right)\frac{\partial y}{\partial t} + \frac{\partial u}{\partial Z} + \left\{\frac{y}{B_A} + \frac{(1-y)}{B_B}\right\}\frac{\partial \ell n P}{\partial t} = 0 \qquad (8)$$

Using the definition

$$B \equiv \frac{B_A}{B_B} \qquad (9)$$

equation (8) may be written

$$(1-B)\frac{\partial y}{\partial t} + B_A\frac{\partial u}{\partial Z} + \{y + B(1-y)\}\frac{\partial \ell n P}{\partial t} = 0 \qquad (10)$$

An important relation expressing continuity is obtained by adding equation (6) X B_A and equation (7) X B_B .

$$\{u(B_A - B_B)\}\frac{\partial y}{\partial Z} + \{B_A y + B_B(1-y)\}\frac{\partial u}{\partial Z} + \frac{\partial \ell n P}{\partial t} - D_L(B_A - B_B)\frac{\partial^2 y}{\partial Z^2} = 0$$

which simplifies to

$$\frac{\partial}{\partial Z}\left\{ \left(B_A y + B_B(1-y)\right)u - \mathcal{D}_L(B_A - B_B)\frac{\partial y}{\partial Z} \right\} = -\frac{\partial \ell n P}{\partial t} \qquad (11)$$

or

$$B_B \frac{\partial}{\partial Z}\left\{ \left(1-(1-B)\right)u + \mathcal{D}_L(1-B)\frac{\partial y}{\partial Z} \right\} = -\frac{\partial \ell n P}{\partial t} \qquad (12)$$

Equations (11) or (12) may be integrated between any two points on the column. When there are no discontinuities in B_A, B_B or u between the points Z_1 and Z_2 ,

$$\left(1-(1-B)y_2\right)u_2 - \left(1-(1-B)y_1\right)u_1 + \mathcal{D}_L(1-B)\left\{\left(\frac{\partial y}{\partial Z}\right)_2 - \left(\frac{\partial y}{\partial Z}\right)_1\right\}$$

$$= -\frac{\partial \ell n P}{\partial t}(Z_2 - Z_1) \qquad (13)$$

This integration may be carried across discontinuities (such as the end of the column or a feed injection point within the column) by matching the flow velocities on each side of the discontinuity. Boundary conditions may be provided by moving or fixed pistons (defining flow at that point), or by open or closed valves. Care must be taken in matching concentrations at the ends of a column since the concentration of flow exiting the column will in general NOT be equal to the concentration within the receiving volume.

When the dispersion term is neglected and pressure is constant during an interval, equation (13) simplifies to

$$\left(1-(1-B)y_2\right)u_2 = \left(1-(1-B)y_1\right)u_1 \qquad (14)$$

valid for no discontinuities in the column between points Z_1 and Z_2 .

The characteristic equation for propagation of concentration wavefronts is derived by subtracting equation (7) X y from equation (6) X $(1-y)$:

$$\left\{\frac{(1-y)}{B_A} + \frac{y}{B_B}\right\}\frac{\partial y}{\partial t} + u\frac{\partial y}{\partial Z} + \left\{\frac{1}{B_A} - \frac{1}{B_B}\right\} y(1-y)\frac{\partial \ell n P}{\partial t} = \mathcal{D}_L \frac{\partial^2 y}{\partial Z^2} \qquad (15)$$

or $$\frac{\partial y}{\partial t} + \frac{B_A B_B}{y B_A + (1-y) B_B} \left\{ u \frac{\partial y}{\partial Z} - D_L \frac{\partial^2 y}{\partial Z^2} \right\} = \frac{(B_A - B_B) y (1-y)}{B_A y + B_B (1-y)} \frac{\partial \ell n P}{\partial t}$$

$$\frac{\partial y}{\partial t} + \frac{B_A}{1-(1-B)y} \left\{ u \frac{\partial y}{\partial Z} - D_L \frac{\partial^2 y}{\partial Z^2} \right\} = - \frac{(1-B) y (1-y)}{1-(1-B)y} \frac{d \ell n P}{dt} \qquad (16)$$

Defining the velocity of the characteristics

$$\frac{dZ}{dt} \equiv \frac{B_A u}{1-(1-B)y} = \frac{B_A B_B u}{B_A y + B_B (1-y)} \qquad (17)$$

and the total time derivative for concentration along a characteristic

$$\frac{dy}{dt} \equiv \frac{\partial y}{\partial t} + \frac{dZ}{dt} \frac{\partial y}{\partial Z} \qquad (18)$$

equation (16) reduces to

$$\frac{dy}{dt} = - \frac{(1-B) y (1-y)}{1-(1-B)y} \frac{d \ell n P}{dt} + \frac{D_L B_A}{1-(1-B)y} \frac{\partial^2 y}{\partial Z^2} \qquad (19)$$

When dispersion is neglected,

$$\frac{dy}{dt} = \frac{(1-B) y (1-y)}{1-(1-B)y} \frac{d \ell n P}{dt} \qquad (20)$$

More general TCPSA cycles can be considered by introducing a temperature gradient

$$T = T(Z)$$

but retaining the approximation of local isothermality.

$$\left(\frac{\partial T}{\partial t} \right)_Z = 0$$

The adsorption isotherms are strongly temperature sensitive

$$B_i = B_i(T) \tag{21}$$

Introducing temperature effects through the ideal gas law, with corresponding generalization of equations (6) and (7), equation (11) without dispersion generalizes to

$$\frac{d\ell nP}{dt} + T(Z)\frac{\partial}{\partial Z}\left\{\frac{u}{T}\left[B_A(T(Z))y + B\,(T(Z))(1-y)\right]\right\} \tag{22}$$

When the temperature distribution T(z) is given, boundary conditions on u are defined by prescribed periodic piston motions, and boundary conditions on y for gas entering the column are known, equation (22) can be integrated to describe the generalized Stirling cycle. Equation (22) in the limit is the basis of the idealized Schmidt model of the Stirling cycle.

Cycle Analysis

In the absence of dispersion, concentration will be constant on each characteristic when pressure is constant. Equation (20) can be integrated directly to give changes in concentration corresponding to a change in pressure, for zero dispersion:

$$\frac{y_1}{y_2}\left[\frac{1-y_2}{1-y_1}\right]^{\beta} = \left[\frac{P_2}{P_1}\right]^{1-\beta} \tag{23}$$

In this one-dimensional model, the normalization assumption is made that the cross-sectional area of any free volume connected to either end of the column is equal to the free flow cross-section area of the adsorbent column (i.e., its voidage). The free volume may be the displacement chamber of a piston, whose actual area and stroke are thus scaled to column dimensions. Take the position of a stationary piston to be $Z = Z_p$, and the adjacent end of the column to be at $Z = Z_c$. The composition in the piston chamber is $y = y_0$. For an expansion step taken while this piston is stationary (i.e., the column is pressurized from the other end), and with dispersion neglected, equations (13) and (17) can be combined with a flow and concentration matching condition at the end of the column to give the motion of a characteristic within the column:

$$\frac{dz}{dt} = -\frac{\beta_A\beta_B}{\{\beta_A y + \beta_B(1-y)\}^2}\frac{d\ell nP}{dt}\left[(Z-Z_c)-(Z_p-Z_c)\left(\beta_A y_0+\beta_B(1-y_0)\right)\right] \tag{24}$$

Substituting equation (20) into (24) gives

$$\frac{dz}{dy} = \frac{\beta}{(1-\beta)}\frac{(Z-Z_0)-(Z_p-Z_0)\left(\beta_A y_0+\beta_B(1-y)\right)}{\left(1-(1-\beta)y\right)(1-y)} \tag{25}$$

which integrates to

$$\frac{(Z_2-Z_0)-(Z_p-Z_0)\left(\beta_A y_0+\beta_B(1-y_0)\right)}{(Z_1-Z_0)-(Z_p-Z_0)\left(\beta_A y_0+\beta_B(1-y_0)\right)} = \left(\frac{y_2}{y_1}\right)^{\frac{\beta}{1-\beta}}\left(\frac{(1-y_1)}{(1-y_2)}\right)^{\frac{1}{1-\beta}}\left(\frac{1-(1-\beta)y_2}{1-(1-\beta)y_1}\right) \tag{26}$$

for the same pressure change as equation (23).

By moving both pistons independently, it is possible to achieve pressure changes while having zero flow at a point Z' within the column, i.e.

The necessary motion of one piston at Z_p will be derived, consistent with the above condition, and in the absence of dispersion. From (13) for the piston chamber and the column

$$u_0 - \dot{Z}_p = -\frac{d\ell nP}{dt}(Z_0 - Z_p)$$

and

$$u_0\left[B_A y_0 + B_B(1-y_0)\right] = \frac{d\ell nP}{dt}(Z' - Z_0)$$

which rearrange to

$$\dot{Z}_p = \frac{d\ell nP}{dt}\left[\frac{Z'-Z}{B_A y_0 + B_B(1-y_0)} - (Z_p - Z_0)\right] \qquad (27)$$

whose integral is

$$\frac{Z_{p_1} - Z_0 - \frac{Z'-Z_0}{B_B}}{Z_{p_2} - Z_0 - \frac{Z'-Z_0}{B_B}} = \frac{P_2}{P_1} \qquad (28)$$

For a constant pressure dispersion free step over an interval between column discontinuities

$$(1-(1-B)y_2)u_2 = (1-(1-B)y_1)u_1 \qquad (14)$$

Dispersion will be most important when concentration gradients are most steep. The dispersion free theory predicts formation of shock waves when feed which is rich in the preferentially adsorbed "heavy" component flows into a depleted zone of the column. The shock wave will be modified by dispersion to approximate the constant pattern wavefront behaviour observed under steady state flow conditions of heavy component feed flowing far along very long initially unloaded columns. For linear isotherms, with a single adsorbed ("heavy") component with an inert carrier, the following equation was derived for the constant pattern wavefront under asymptotic steady state conditions in an infinitely long column:

$$\frac{y-\frac{y_0}{2}}{\frac{y_0}{2}} = \tanh\left[\frac{u_0(1-B)y_0 Z}{2D_L}\right] \qquad (29)$$

where y_0 is the feed concentration, and $y = 0$ far ahead of the wavefront. After selecting upstream and downstream tolerances on concentration, equation (29) can be used to estimate the effective width of the constant patterm transfer zone. For more general isotherms and for non-equilibrium adsorbent response, more general expressions for the constant pattern wavefront are available in the literature, as reviewed by Ruthven (reference R1)

The propagation velocity for the idealized constant pattern wavefront of equation (29) is simply

$$\frac{dZ}{dt} = B_A u \qquad (30)$$

Equations (29) and (30) were derived from equations (10) and (11), under the above assumptions of constant pressure and asymptotic steady flow into an initially unloaded column.

The above relations enable analysis of simplified cycles, broken down into discrete steps of

(1) compression (with velocity held zero either at a some fixed point outside the column at a stationary piston or closed valve, or at some intermediate station within the column),

(2) constant pressure "feed" and product delivery,

(3) expansion (again with zero velocity held at a point outside or inside the column), and

(4) constant pressure "purge".

The cycle may be inverted by exchanging the compression and expansion steps, to produce purified "heavy" rather than "light" fraction. The basic principle of these general cycles can be displayed in simple solutions by having two pistons (one at each end of the column) following out-of-phase trapezoidal waveforms (approximating more typical sinusoids) to meet the simplifying condition that flow is held zero at some (unique) point during intervals of pressure change, and pressure is held constant during other intervals of flow through the entire system. Such cycles can be analyzed conveniently by considering one piston at a time, in combination with the pressure regime determined

jointly with the other piston whose trajectory may be derived subsequently.

In conventional PSA cycles, the point of zero velocity during compression or expansion is located at an end of the column by the closure of a directional valve with minimal dead volume between the valve and the column, so that $Z_0 = Z_p$ in equation (26).

In the piston operated flow-controlled PSA cycles, a free volume may be present during compression or expansion according to the position of a stationary piston defining the point of zero flow, or both pistons may move simultaneously (together during compression and apart during expansion) with unavoidable free volume in each cylinder as a point of zero flow is maintained within the column.

Following the standard terminology of the Stirling cycle, displacements of the "expansion" cylinder lead those of the "compression" cylinder by a phase angle between 0 and 180 degrees. In the idealization of perfect separation performance, a TCPSA system can be arranged to deliver pure light component to the expansion cylinder ($y_E = 0$) and pure heavy component to the compression cylinder ($y_C = 1$). Heat will also be transported from the expansion cylinder to the compression cylinder, with energy conversion across any imposed static temperature gradient according to the principle of the Stirling cycle.

Simple closed periodic solutions can be obtained in the above limit of ideal purification ($y_E = 0$ or $y_C = 1$), since the concentration boundary conditions at the ends of the column become trivial. With non-ideal purification, the concentration within a free volume at the end of the column will vary with mixing of variable concentration effluent from the column, and the boundary conditions must be determined by iteration within the total solution.

We will now investigate simple flow-regulated cycles in the limit of perfect purification, considering the motion of only one piston with a prescribed regime of pressure changes (determined in cooperation with the other piston). We define the case of considering an expansion cylinder producing pure light product ($y_E = 0$) as the "normal" cycle, and the opposite case of considering a compression cylinder producing pure heavy component ($y_C = 1$) as the "inverse" cycle. An actual system may approximate either the normal or inverse cycles, or may combine both if arranged to produce both light and heavy products simultaneously.

We further define a Type I flow-controlled cycle as an idealized

normal or inverse cycle in which the piston under consideration moves only when the pressure is constant, and is stationary during pressure changes. We define a Type II cycle as one in which both pistons move during pressure changes to maintain zero flow velocity at a selected point $Z = Z'$ during compression, and at another point (intercepted by the same charateristic) during expansion.

In a first analysis of a TCPSA steam reformer, the temperature gradient along the adsorbent bed may be neglected by assuming an effective lumped values for the distribution coefficients, or equivalently adjusting the axial length scale to compensate for thermal dependence of the isotherm slopes. In the steam reformer, it is desired to produce synthesis gas as a pure light component, trapping steam as the heavy component. This may be achieved by a "normal Type I" cycle.

The criteria for producing a pure light product at the expansion cylinder are:

1) no breakthrough of the heavy component into the expansion cylinder. The column is designed to be longer than the greatest penetration distance of feed entering the column during the cycle, plus the length of the mass transfer zone.

2) under steady state periodic operation, the characteristics migrate progressively AWAY from the product delivery point (at the expansion cylinder end of the column), reflecting the physical fact that the heavy component of the feed is rejected by the column while the light component may pass through as product. Maximum theoretical productivity is achieved when the rate of product withdrawal is high enough to bring the net cyclic migration of a reference characteristic to zero.

The normal Type I cycle comprises the four steps shown in Figure A1 of compression, feed, expansion, and purge. We begin the cycle with compression, starting from pressure P_1 and concentration y_1 at a point Z_1, and proceeding to P_2, y_2, Z_2. Neglecting dispersion,

$$\frac{P_1}{P_2} = \left(\frac{y_2}{y_1}\right)^{\frac{1}{1-B}} \left(\frac{1-y_1}{1-y_2}\right)^{\frac{B}{1-B}} \tag{31}$$

$$\frac{Z_2}{Z_1} = \frac{1}{G_{12}} \tag{32}$$

where

$$G_{12} \equiv \left(\frac{y_1}{y_2}\right)^{\frac{B}{1-B}} \left(\frac{1-y_2}{1-y_1}\right)^{\frac{1}{1-B}} \left(\frac{1-(1-B)y_1}{1-(1-B)y_2}\right) \tag{33}$$

During the feed step of duration Δt, the expansion piston moves its stroke ℓ_E (piston area normalized equal to column voidage area) while a volume ℓ_{PROD} X piston area $= \ell_{PROD}$ X column voidage area) of product is delivered. We may somewhat improperly neglect dispersion and shock effects to obtain

$$\frac{Z_2 - Z_3}{\Delta t} = -\frac{B_A(\ell_E + \ell_{PROD})}{\Delta t} \frac{1-(1-B)y_E}{(1-(1-B)y_2)^2} \tag{34}$$

An alternative approximation is to assume a constant pattern wavefront, such that

$$\frac{Z_2 - Z_3}{\Delta t} = -\frac{B_A(\ell_E + \ell_{PROD})}{\Delta t} \frac{1-(1-B)y_E}{1-(1-B)y_F} \tag{35}$$

where y_F is the feed concentration. Since dispersion is included in the derivation of (30), (35) gives displacements of trajectories of constant concentration, which in general are not coincident with the characteristics.

During expansion from $Z_0 - \ell_E$,

$$\frac{Z_4 + Z_0\left(B_A y_E + B_B(1-y_E)\right)}{Z_3 + Z_0\left(B_A y_E + B_B(1-y_E)\right)} = \frac{Z_4 + Z_0 B_B}{Z_3 + Z_0 B_B} = G_{12} \tag{36}$$

During purge,

$$Z_5 = Z_4 + \frac{B_A \ell_E}{(1-(1-B)y_1)^2} \tag{37}$$

Selecting (34) for convenience as the expression for the feed step, the migration of the characteristics is given by

$$\Delta Z = Z_5 - Z_1$$

$$= \ell_E \left[B_B(G_{12}-1) - \frac{B_A G_{12}}{(1-(1-B)y_2)^2} + \frac{B_A}{(1-(1-B)y_1)^2} \right] - \frac{B_A \ell_{PROD} G_{12}}{(1-(1-B)y)^2} \tag{38}$$

A product purity condition is

$$\Delta Z > 0$$

In the limit that the heavy component is a small impurity, $y_1 \simeq 0$ and $y_2 \simeq 0$. Then

$$\frac{P_1}{P_2} \simeq \left(\frac{y_2}{y_1}\right) \frac{1}{1-B} \tag{39}$$

and

$$G_{12} \simeq \left(\frac{y_1}{y_2}\right)^{\frac{B}{1-B}} \simeq \left(\frac{P_2}{P_1}\right)^B \tag{40}$$

Hence

$$\Delta Z \simeq \ell_E (B_B - B_A) \left[\left(\frac{P_2}{P_1}\right)^B - 1 \right] - \ell_{PROD} B \left(\frac{P_2}{P_1}\right)^B \tag{41}$$

To obtain complete separation of a trace preferentially adsorbed component, with $(\Delta Z > 0)$

$$\frac{\ell_{PROD}}{\ell_E} < \frac{B_B - B_A}{B} \left[1 - \left(\frac{P_1}{P_2}\right)^B \right] \tag{42}$$

FIGURE B1

FLOW - CONTROLLED PSA CYCLE: NORMAL TYPE I

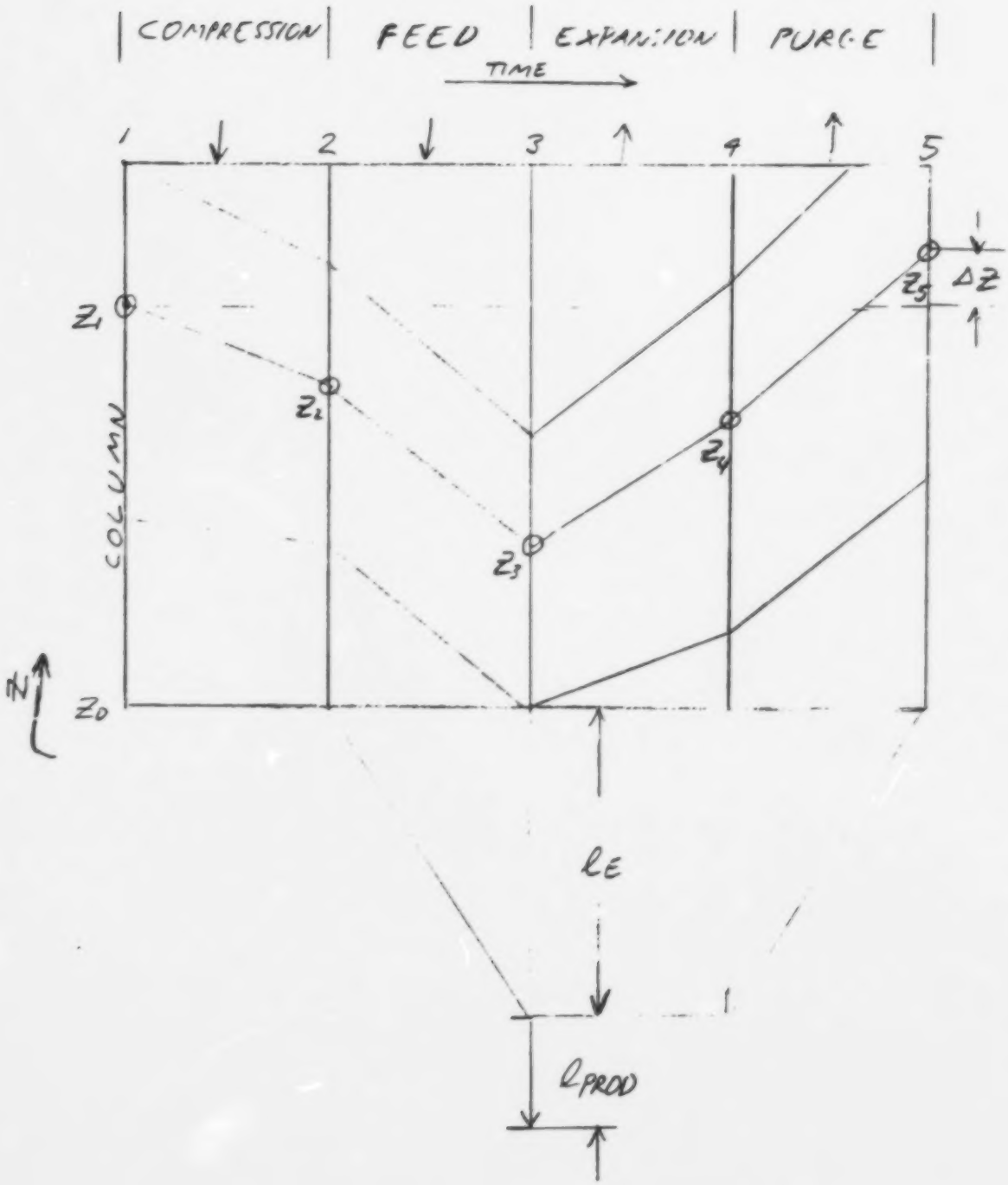

ANNEX C: EXPERIMENTAL RUN LOG.

The following table is a summary of the operating conditions for all experimental runs completed and whether or not water separation was detected. Runs marked "inconclusive" in the separation column indicate water was separated though the separation was not definite enough to declare conclusively that it did occur. Separation was conclusively detected for all runs indicated.

In general, inconclusive or no results were obtained for runs 032186-01 to 040886-04. These runs were characterized by a great deal of difficulty in detecting and measuring the water in the test rig. It is thought that the major reason for this was a loss of water in the test rig due to condensation.

From runs 040886-05 to 041886-01 generally good results were obtained with only a few problems occurring in runs 041586-01, 041686-01 and 041786-01. In this group of runs, separation was clearly observed except for the three runs noted. It is believed however, that some water was still condensing as the water peaks were very weak (as seen in Figures 18 to 21) relative to the nitrogen peaks. This belief is supported by the results of run 041786-01 were water was not observed until the temperature was increased to 800 degrees C.

From runs 042286-01 to 051386-01 wear and tear on the test rig began to have an effect and the results were generally poor. Excessive seal wear and a total seizure of the test rig resulting in extensive damage to the cylinders made it difficult to maintain the gas charge in the test rig. Because of the pressure losses that occurred during these experiments, the test conditions could not be maintained and the results were deemed inconclusive.

In summary, positive separation of the water was detected in 10 of the 49 runs done. Of the remaining runs, difficulties with the test rig rendered the results inconclusive. It is encouraging to note however, that in none of the runs was water separation in the wrong direction observed.

TABLE C1: SUMMARY OF EXPERIMENTAL RUN CONDITIONS AND RESULTS

EXPERIMENTAL RUNS SUMMARY

Experiment Number	Adsorbent Type	Temp. oC	Pressure psig	Water ml	Stirling Cycle mode	Speed rpm	Separation
032186-01	13x	500	20	0.10	Heat Pump	4	inconclusive
032186-02	13x	500	20	0.05	Heat Pump	4	inconclusive
032486-01	13x	400	20	0.20	Heat Pump	8	inconclusive
032486-02	13x	400	20	0.20	Heat Pump	8	no
032686-01	Alumina	120	20	0.20	Heat Pump	5	inconclusive
040286-01	Alumina	400	50	0.10	Heat Pump	5	inconclusive
040286-02	Alumina	400	80	0.10	Heat Pump	10	inconclusive
040386-01	Alumina	400	50	0.25	Heat Pump	5	inconclusive
040386-02	Alumina	400	150	0.25	Heat Pump	5	inconclusive
040486-01	Alumina	400	50	0.03	Heat Pump	5	no
040486-02	Alumina	400	50	0.02	Heat Pump	5	no
040786-01	Alumina	400	150	0.02	Heat Pump	5	no
040786-02	Alumina	400	100	0.02	Heat Pump	5	no
040786-03	Alumina	400	100	0.04	Heat Pump	5	inconclusive
040886-01	Alumina	400	100	0.04	Heat Pump	5	no
040886-02	Alumina	400	100	0.04	Heat Pump	5	no
040886-03	Alumina	400	50	0.04	Heat Pump	5	inconclusive
040886-04	Alumina	400	100	0.10	Heat Pump	5	inconclusive
040886-05	Alumina	400	100	0.05	Heat Pump	5	inconclusive
						15	yes
						30	yes
					Engine	30	inconclusive
040986-01	Alumina	400	100	0.20	Heat Pump	10	inconclusive
040986-02	Alumina	500	100	0.10	Heat Pump	10	yes
041086-01	Alumina	500	100	0.05	Heat Pump	10	yes
					Engine		yes
					Heat Pump		yes
041186-01	Alumina	600	100	0.05	Heat Pump	10	yes
					Engine		yes
041586-01	Alumina	400	100	0.10	Heat Pump	10	no
041686-01	Alumina	400	100	0.10	Heat Pump	10	no

TABLE C1 - CONTINUED

Experiment Number	Adsorbent Type	Temp. oC	Pressure psig	Water ml	Stirling Cycle mode	Speed rpm	Separation
041786-01	Alumina	600	100	0.17	Heat Pump	10	no
		800					yes
041886-01	Alumina	800	100	0.05	Heat Pump	10	yes
042286-01	Alumina	800	100	0.10	Heat Pump	10	inconclusive
					Engine		inconclusive
042486-01	Alumina	400	150	0.05	Heat Pump	10	no
042486-02	Alumina	400	150	0.15	Heat Pump	10	no
						20	no
042586-01	Alumina	500	150	0.10	Heat Pump	10	no
042586-02	Alumina	500	150	0.10	Heat Pump	10	inconclusive
042886-01	Alumina	600	100	0.10	Heat Pump	10	inconclusive
						20	inconclusive
042886-02	Alumina	400	200	0.05	Heat Pump	10	no
042986-01	Alumina	500	100	0.10	Heat Pump	10	inconclusive
			(35% CO2)				
043086-01	Alumina	500	100	0.15	Heat Pump	10	no
			(25% CO2)				
050106-01	Alumina	500	100	0.10	Heat Pump	10	yes
			(35% CO2)				
050206-01	Alumina	500	100	0.10	Heat Pump	10	inconclusive
			(25% CO2)				
050506-01	Alumina	400	100	0.07	Heat Pump	10	inconclusive
			(25% CO2)				
050606-01	Alumina	500	100	0.05	Heat Pump	10	inconclusive
			(10% CO2)				
050706-01	Alumina	500	100	0.05	Heat Pump	10	inconclusive
			(10% CO2)				
050806-01	Alumina	500	100	0.05	Heat Pump	10	no
050806-02	Alumina	500	100	0.10	Heat Pump	10	no
050906-01	Alumina	500	100	0.10	Heat Pump	10	no
050906-02	Alumina	500	100	0.05	Heat Pump	10	no
051206-01	Alumina	500	100	0.05	Heat Pump	10	no
051206-02	Alumina	500	100	0.10	Heat Pump	10	no
051306-01	Alumina	600	100	0.05	Heat Pump	10	inconclusive

ANNEX D

STIRLING CYCLE ANALYSIS

The reactor configuration shown in Figure D1 includes a steam reforming TCPSA module operating at high temperature, integrated directly with a Stirling cycle engine drawing heat from an adjacent F.T reactor. As the steam reforming reaction is endothermic, the steam reforming TCPSA stage must act as a Stirling cycle heat pump. The syngas conversion reaction is exothermic, and a heat exchanger provides F.T. reactor heat to the Stirling cycle engine. As only a portion of the exothermic heat of syngas conversion is available as input to the cool end of the steam reforming heat pump, additional heat must be provided to make up the endothermic steam reforming heat load.

The engine and heat pump displacers are driven by suitable linear actuators to cause cyclic gas flows in the engine regenerator and heat pump regenerator. When the reciprocating displacements and phases of the pistons are properly selected, the exothermic heat of syngas conversion will partly be converted to pneumatic energy through the Stirling engine function, and this pneumatic energy will directly drive the heat pump function to lift the useful remainder of this heat to steam reforming temperatures. The heat pump function is the load on the engine function. The effect of loading the engine section with the heat pump section is to reduce the amplitude of pressure excursions in the working spaces. In this configuration, two Stirling cycles (engine and heat pump) are integrated to use the same pressure regime, although they work across different temperature ranges. This configuration was modelled using the so-called Schmidt model, whose assumptions are recited in Section 3.4.

An excellent description of the Schmidt model as applied to simple Stirling cycle machines is provided in Appendix A of "Stirling Engines", by G.T. Reader and C. Hooper, published by E. & F.N. Spon, London, 1983. This model assumes perfect heat exchange, locally isothermal conditions at each point within the Stirling machine working space, ideal gas law behaviour, and sinusoidal piston motions. As the volumes associated with pistons are prescribed kinematically, pressure (assumed to be equal at all positions at each instant) can be determined by direct integration, since the number of moles in the total working space is also assumed to be constant. Knowing the time variation of pressure, mass flows, compression or expansion work, and external heat exchanges (equal to isothermal work) can be calculated almost trivially.

The following analysis extends the standard Schmidt model by generalizing to two displacers (pistons 1 and 2) associated with one compression piston (piston 3). By

assuming equal diameter of the three pistons, their displacements are normalized to their strokes. The presence of adsorbent and catalyst is accomodated in this first order model by a crude allowance of extra dead volume. External gas exchanges (feed and product condensation or removal) are neglected.

The computer model based on the following analysis was used to explore a wide range of possible piston phase and displacement relationships (with the three temperatures of steam reforming, F.T heat recovery, and heat rejection fixed). As expected, satisfactory engine and heat pump operation could only be obtained with a limited range of phase relationships, which was narrowed further by the requirement to perform pressure swing adsorption separation in the steam reforming stage, as discussed in Section 3.4.

Results of this analysis for a satisfactory compound steam reforming/syngas conversion compound TCPSA reactor are presented in Figure 6, and in Table D1 of this annex.

FIGURE D1

SCHEMATIC FOR STIRLING CYCLE NOMENCLATURE

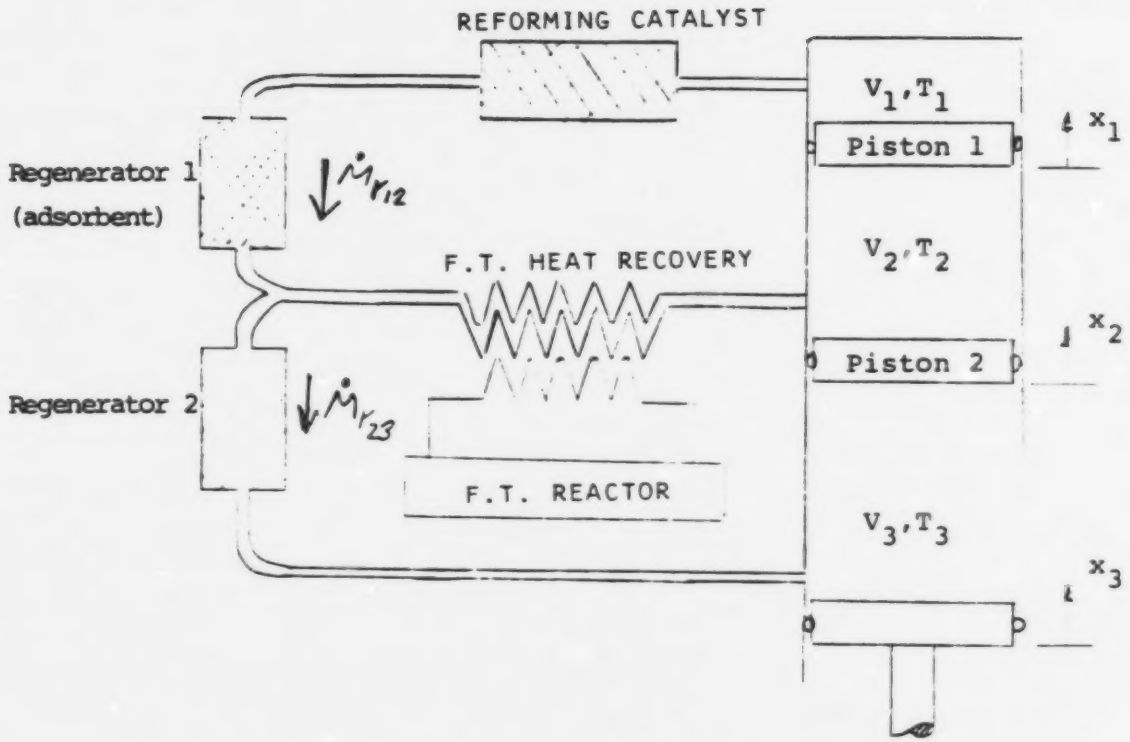

NOMENCLATURE

V_i	=	volume of space "i"
ϕ	=	crank angle ($\phi = 0$ when piston 1 is at top dead centre)
α_i	=	phase angle of piston "i" relative to piston 1
T_i	=	temperature of space "i"
p	=	pressure
M_i	=	mass in space "i"
R	=	gas constant
W	=	work
x_i	=	stroke of piston "i"
$\dot{M}_i$	=	mass flow into space i" or thro' regenerator "i"

Subscripts

1, 2, 3	refers to	volumes 1, 2 & 3
02, 03	" "	overlap volumes 2 & 3
D1, D2, D3	" "	dead " 1, 2 & 3
S1, S2, S3	" "	swept " 1, 2 & 3
r_{12}, r_{23}	" "	regenerators between volumes 1&2, and 2&3.

Notes:

1. V_{01} & V_{02} are input parameters specifying the amount of piston overlap that may occur. The equations for V_{01} & V_{02} given on page D7 are conditions that the specified values must meet if positive overlaps are specified. Evaluation of these equations yields the maximum values that may be specified to ensure piston collisions do not occur.

2. Regenerator mass flows are calculated as:

$$\dot{M}_{r_{12}} = -\left(\dot{M}_1 + \dot{M}_{D1}\right)$$

$$\dot{M}_{r_{23}} = \left(\dot{M}_3 + \dot{M}_{D3}\right)$$

STIRLING CYCLE ANALYSIS

Compound heat engine – heat pump

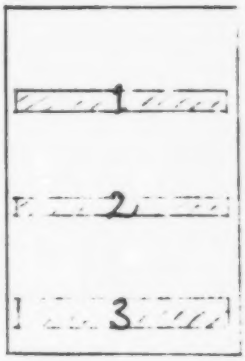

$$V_1 = \tfrac{1}{2} V_{S1}\left(1 - \cos\phi\right) + V_{D1}$$

$$V_2 = \tfrac{1}{2} V_{S1}\left(1 + \cos\phi\right) + \tfrac{1}{2} V_{S2}\left[1 - \cos(\phi - \alpha_2)\right] + V_{D2} + V_{O2}$$

$$V_3 = \tfrac{1}{2} V_{S2}\left[1 + \cos(\phi - \alpha_2)\right] + \tfrac{1}{2} V_{S3}\left[1 - \cos(\phi - \alpha_3)\right] + V_{D3} + V_{O3}$$

now, as before

$$M_T = \frac{P}{R}\left(\frac{V_1}{T_1} + \frac{V_2}{T_2} + \frac{V_3}{T_3}\right)$$

$$= \frac{P}{R}\left\{\frac{\tfrac{1}{2} V_{S1}(1-\cos\phi)}{T_1} + \frac{\tfrac{1}{2} V_{S1}(1+\cos\phi) + \tfrac{1}{2} V_{S2}\left[1-\cos(\phi-\alpha_2)\right]}{T_2}\right.$$

$$+ \frac{\tfrac{1}{2} V_{S2}\left[1+\cos(\phi-\alpha_2)\right] + \tfrac{1}{2} V_{S3}\left[1-\cos(\phi-\alpha_3)\right]}{T_3} + \left(\frac{V_{O2}}{T_2} + \frac{V_{O3}}{T_3}\right)$$

$$\left. + \left(\frac{V_{D1}}{T_1} + \frac{V_{D2}}{T_2} + \frac{V_{D3}}{T_3}\right)\right\}$$

$$= \frac{P}{2R}\left\{\left(-\frac{V_{S1}}{T_1}+\frac{V_{S1}}{T_2}\right)\cos\phi+\left(-\frac{V_{S2}}{T_2}+\frac{V_{S2}}{T_3}\right)\cos(\phi-\alpha_2)-\frac{V_{S3}}{T_3}\cos(\phi-\alpha_3)\right.$$

$$\left.+\left(\frac{V_{S1}}{T_1}+\frac{V_{S1}}{T_2}+\frac{V_{S2}}{T_2}+\frac{V_{S1}}{T_3}+\frac{V_{S3}}{T_3}\right)+2\left(\frac{V_{O2}}{T_2}+\frac{V_{O3}}{T_3}\right)+2\left(\frac{V_{D1}}{T_1}+\frac{V_{D2}}{T_2}+\frac{V_{D3}}{T_3}\right)\right\}$$

$$= \frac{P}{2R}\left\{V_{S1}\left(\frac{-T_2+T_1}{T_1T_2}\right)\cos\phi+V_{S2}\left(\frac{-T_2+T_3}{T_2T_3}\right)\cos(\phi-\alpha_2)-V_{S3}\left(\frac{1}{T_3}\right)\cos(\phi-\alpha_3)\right.$$

$$+V_{S1}\left(\frac{T_2+T_1}{T_1T_2}\right)+V_{S2}\left(\frac{T_3+T_2}{T_2T_3}\right)+V_{S3}\left(\frac{1}{T_3}\right)+2\left(\frac{V_{O2}}{T_2}+\frac{V_{O3}}{T_3}\right)$$

$$\left.+2\left(\frac{V_{D1}}{T_1}+\frac{V_{D2}}{T_2}+\frac{V_{D3}}{T_3}\right)\right\}$$

$$M_T = \frac{P}{2R}\left\{V_{S1}\left(\frac{-T_2+T_1}{T_1T_2}\right)\cos\phi+V_{S2}\left(\frac{-T_3+T_2}{T_2T_3}\right)(\cos\phi\cos\alpha_2+\sin\phi\sin\alpha_2)\right.$$

$$-V_{S3}\left(\frac{1}{T_3}\right)(\cos\phi\cos\alpha_3+\sin\phi\sin\alpha_3)+V_{S1}\left(\frac{T_1+T_2}{T_1T_2}\right)+V_{S2}\left(\frac{T_3+T_2}{T_2T_3}\right)+V_{S3}\left(\frac{1}{T_3}\right)$$

$$\left.+2\left(\frac{V_{O2}}{T_2}+\frac{V_{O3}}{T_3}\right)+2\left(\frac{V_{D1}}{T_1}+\frac{V_{D2}}{T_2}+\frac{V_{D3}}{T_3}\right)\right\}$$

Compound engine analysis

$$M_T = \frac{P}{2R}\left\{\left[V_{S1}\left(\frac{T_2+T_1}{T_1T_2}\right) + V_{S2}\left(\frac{T_3+T_2}{T_2T_3}\right)\cos\alpha_2 - V_{S3}\left(\frac{1}{T_3}\right)\cos\alpha_3\right]\cos\phi\right.$$

$$+ \left[V_{S2}\left(\frac{T_3+T_2}{T_2T_3}\right)\sin\alpha_2 - V_{S3}\left(\frac{1}{T_3}\right)\sin\alpha_3\right]\sin\phi$$

$$+ \left.\left[V_{S1}\left(\frac{T_2+T_1}{T_1T_2}\right) + V_{S2}\left(\frac{T_3+T_2}{T_2T_3}\right) + V_{S3}\left(\frac{1}{T_3}\right) + 2\left(\frac{V_{O2}}{T_2}+\frac{V_{O3}}{T_3}\right) + 2\left(\frac{V_{D1}}{T_1}+\frac{V_{D2}}{T_2}+\frac{V_{D3}}{T_3}\right)\right]\right.$$

$$M_T = \frac{P}{2R}\left\{A\cos\phi + B\sin\phi + C\right\}$$

Letting $M_T = \frac{C}{2R}$

$$\frac{C}{P} = \left[A\cos\phi + B\sin\phi + C\right]$$

$$= \left[\left(A^2+B^2\right)^{1/2}\cos\left(\phi-\theta\right) + C\right]$$

$\theta = \tan^{-1}\left(\frac{B}{A}\right)$ and letting $\delta = \frac{\left(A^2+B^2\right)^{1/2}}{C}$

$$P = \frac{\frac{C}{C}}{\left[1 + \delta\cos(\phi-\theta)\right]}$$

Compound engine analysis :

$$p = \frac{P_{max}(1-\delta)}{[1+\delta\cos(\phi-\theta)]}$$

now

$$W = \oint p\,dv$$

W_1 : $\quad dv_1 = -\frac{1}{2} v_{s1} \sin\phi\, d\phi$

$$W_1 = \int_0^{2\pi} \frac{-P_{max}(1-\delta)}{[1+\delta\cos(\phi-\theta)]} \cdot \tfrac{1}{2} v_{s1} \sin\phi\, d\phi$$

$$= \left[-\tfrac{1}{2} v_{s1} P_{max}(1-\delta)\right]\left[\frac{2\pi}{\delta}\sin\theta\right]\left[1-\frac{1}{(1-\delta^2)^{\frac{1}{2}}}\right]$$

W_2 : $\quad dv_2 = \frac{1}{2} v_{s1} \sin\phi\, d\phi - \frac{1}{2} v_{s2} \sin(\phi-\alpha_2)\, d\phi$

$$= \tfrac{1}{2} v_{s1} \sin\phi\, d\phi - \tfrac{1}{2} v_{s2}\left[\sin\phi\cos\alpha_2 - \sin\alpha_2\cos\phi\right] d\phi$$

$$= \left[\left(\tfrac{1}{2} v_{s1} - \tfrac{1}{2} v_{s2}\cos\alpha_2\right)\sin\phi + \tfrac{1}{2} v_{s2}\sin\alpha_2\cos\phi\right] d\phi$$

$$= \tfrac{1}{2}\left[\left(v_{s1} - v_{s2}\cos\alpha_2\right)\sin\phi + v_{s2}\sin\alpha_2\cos\phi\right] d\phi$$

$$W_2 = \int_0^{2\pi} \left\{\frac{P_{max}(1-\delta)}{[1+\delta\cos(\phi-\theta)]}\right\} \cdot \tfrac{1}{2}\left[\left(v_{s1} - v_{s2}\cos\alpha_2\right)\sin\phi + v_{s2}\sin\alpha_2\cos\phi\right] d\phi$$

Compound engine analysis

$$W_2 = \left[\tfrac{1}{2} P_{max}(1-\delta)\right]\left\{(V_{s1} - V_{s2}\cos\alpha_2)\int_0^{2\pi} \frac{\sin\phi\, d\phi}{[1+\delta\cos(\phi-\theta)]} + V_{s2}\sin\alpha_2 \int_0^{2\pi} \frac{\cos\phi\, d\phi}{[1+\delta\cos(\phi-\theta)]}\right\}$$

$$= \left[\tfrac{1}{2} P_{max}(1-\delta)\right]\left\{(V_{s1} - V_{s2}\cos\alpha_2)\left(\frac{2\pi\sin\theta}{\delta}\right)\left[1 - \frac{1}{(1-\delta^2)^{\frac{1}{2}}}\right] + V_{s2}\sin\alpha_2 \int_0^{2\pi} \frac{\cos\phi\, d\phi}{1+\delta\cos(\phi-\theta)}\right\}$$

integrating the RH expression as for W_1 :

$$W_2 = \left[\tfrac{1}{2} P_{max}(1-\delta)\right]\left\{(V_{s1} - V_{s2}\cos\alpha_2)\left(\frac{2\pi\sin\theta}{\delta}\right)\left[1 - \frac{1}{(1-\delta^2)^{\frac{1}{2}}}\right] + (V_2\sin\alpha_2)\left(\frac{2\pi\cos\theta}{\delta}\right)\left[1 - \frac{1}{(1-\delta^2)^{\frac{1}{2}}}\right]\right.$$

$$= \left[\tfrac{1}{2} P_{max}(1-\delta)\right]\left[(V_{s1} - V_{s2}\cos\alpha_2)(\sin\theta) + (V_{s2}\sin\alpha_2)(\cos\theta)\right]\left[\frac{2\pi}{\delta}\right]\left[1 - \frac{1}{(1-\delta^2)^{\frac{1}{2}}}\right]$$

$$W_2 = \left[\tfrac{1}{2} P_{max}(1-\delta)\right]\left[\frac{2\pi}{\delta}\right]\left[1 - \frac{1}{(1-\delta^2)^{\frac{1}{2}}}\right]\left[V_{s1}\sin\theta - V_{s2}\sin(\theta-\alpha_2)\right]$$

W_3 : $\quad dV_3 = \tfrac{1}{2} V_{s2}\sin(\phi-\alpha_2)\,d\phi - \tfrac{1}{2} V_{s3}\sin(\phi-\alpha_3)\,d\phi$

$$= \left[\tfrac{1}{2} V_{s2}(\sin\phi\cos\alpha_2 - \sin\alpha_2\cos\phi) - \tfrac{1}{2} V_{s3}(\sin\phi\cos\alpha_3 - \sin\alpha_3\cos\phi)\right] d\phi$$

$$= \tfrac{1}{2}\left[(V_{s2}\cos\alpha_2 - V_{s3}\cos\alpha_3)\sin\phi - (V_{s2}\sin\alpha_2 - V_{s3}\sin\alpha_3)\cos\phi\right] d\phi$$

$$W_3 = \tfrac{1}{2} P_{max}(1-\delta)\int_0^{2\pi}\left[\frac{(V_{s2}\cos\alpha_2 - V_{s3}\cos\alpha_3)\sin\phi - (V_{s2}\sin\alpha_2 - V_{s3}\sin\alpha_3)\cos\phi}{1+\delta\cos(\phi-\theta)}\right] d\phi$$

$$= \left[\tfrac{1}{2} P_{max}(1-\delta)\right]\left\{(V_{s2}\cos\alpha_2 - V_{s3}\cos\alpha_3)\int_0^{2\pi} \frac{\sin\phi\, d\phi}{1+\delta\cos(\phi-\theta)} - (V_{s2}\sin\alpha_2 - V_{s3}\sin\alpha_3)\int_0^{2\pi} \frac{\cos\phi\, d\phi}{1+\delta\cos(\phi-\theta)}\right.$$

Compound engine analysis:

$$W_3 = \left[\tfrac{1}{2} P_{max}(1-\delta)\right]\left\{\left(V_{S2}\cos\alpha_2 - V_{S3}\cos\alpha_3\right)\left(\frac{2\pi\sin\theta}{\delta}\right)\left[1-\frac{1}{(1-\delta^2)^{\frac{1}{2}}}\right]\right.$$

$$\left. - \left(V_{S2}\sin\alpha_2 - V_{S3}\sin\alpha_3\right)\left(\frac{2\pi\cos\theta}{\delta}\right)\left[1-\frac{1}{(1-\delta^2)^{\frac{1}{2}}}\right]\right\}$$

$$= \left(\frac{\pi}{\delta}\right)\left[P_{max}(1-\delta)\right]\left[1-\frac{1}{(1-\delta^2)^{\frac{1}{2}}}\right]\left[\left(V_{S2}\cos\alpha_2 - V_{S3}\cos\alpha_3\right)\sin\theta - \left(V_{S2}\sin\alpha_2 - V_{S3}\sin\alpha_3\right)\cos\theta\right]$$

$$W_3 = \left(\frac{\pi}{\delta}\right)\left(P_{max}\right)\left(1-\delta\right)\left[1-\frac{1}{(1-\delta^2)^{\frac{1}{2}}}\right]\left[V_{S2}\sin(\theta-\alpha_2) - V_{S3}\sin(\theta-\alpha_3)\right]$$

$$W_T = W_1 + W_2 + W_3$$

$$= -\left(\frac{\pi}{\delta}\right)\left(P_{max}\right)\left(1-\delta\right)\left[1-\frac{1}{(1-\delta^2)^{\frac{1}{2}}}\right] V_{S1}\sin\theta$$

$$+ \left(\frac{\pi}{\delta}\right)\left(P_{max}\right)\left(1-\delta\right)\left[1-\frac{1}{(1-\delta^2)^{\frac{1}{2}}}\right]\left[V_{S1}\sin\theta - V_{S2}\sin(\theta-\alpha_2)\right]$$

$$+ \left(\frac{\pi}{\delta}\right)\left(P_{max}\right)\left(1-\delta\right)\left[1-\frac{1}{(1-\delta^2)^{\frac{1}{2}}}\right]\left[V_{S2}\sin(\theta-\alpha_2) - V_{S3}\sin(\theta-\alpha_3)\right]$$

$$W_T = -\left(\frac{\pi}{\delta}\right)\left(P_{max}\right)\left(1-\delta\right)\left[1-\frac{1}{(1-\delta^2)^{\frac{1}{2}}}\right]\left[V_{S3}\sin(\theta-\alpha_3)\right]$$

Compound engine - overlap volumes

V_{02}: at point of contact (pistons 1 & 2) $V_2 = \emptyset$

$$\therefore \quad V_2 = \tfrac{1}{2} V_{S1}(1-\cos\phi) + \tfrac{1}{2} V_{S2}\left[1+\cos(\phi-\alpha_2)\right] + V_{02} = 0$$

$$\begin{aligned} V_{02} &= -\min\left\{\tfrac{1}{2} V_{S1}(1-\cos\phi) + \tfrac{1}{2} V_{S2}\left[1+\cos(\phi-\alpha_2)\right]\right\} \\ &= -\min\left\{\tfrac{1}{2} V_{S1} - \tfrac{1}{2} V_{S1}\cos\phi + \tfrac{1}{2} V_{S2} + \tfrac{1}{2} V_{S2}\cos(\phi-\alpha_2)\right\} \\ &= -\min\left\{\tfrac{1}{2} V_{S1} + \tfrac{1}{2} V_{S2} - \tfrac{1}{2} V_{S1}\cos\phi + \tfrac{1}{2} V_{S2}\cos\phi\cos\alpha_2 + \tfrac{1}{2} V_{S2}\sin\phi\sin\alpha_2\right\} \\ &= -\tfrac{1}{2}\min\left\{(V_{S1}+V_{S2}) + (V_{S1}\cos\alpha_2 - V_{S1})\cos\phi + V_{S2}\sin\alpha_2\sin\phi\right\} \\ &= -\tfrac{1}{2}\min\left\{(V_{S1}+V_{S2}) + (A^2+B^2)^{1/2}\cos(\phi-\beta)\right\} \end{aligned}$$

Where $A = V_{S2}\cos\alpha_2 - V_{S1}$

$B = V_{S2}\sin\alpha_2$

$\beta = \tan^{-1}\left(\frac{B}{A}\right)$

the above expression is a min when $\cos(\phi-\beta) = -1$

$$\therefore \quad V_{02} = -\tfrac{1}{2}\left[(V_{S1}+V_{S2}) - \left(V_{S_2}^2 - 2V_{S_1}V_{S_2}\cos\alpha_2 + V_{S_1}^2\right)^{1/2}\right]$$

V_3:

$$\begin{aligned} V_{03} &= -\tfrac{1}{2}\min\left\{V_{S2} - V_{S_2}\cos\phi\cos\alpha_2 - V_{S2}\sin\phi\sin\alpha_2 + V_{S3} + V_{S3}\cos\phi\cos\alpha_3 + V_{S3}\sin\phi\sin\right. \\ &= -\tfrac{1}{2}\min\left\{(V_{S2}+V_{S3}) + (V_{S3}\cos\alpha_3 - V_{S2}\cos\alpha_2)\cos\phi + (V_{S3}\cos\alpha_3 - V_{S3}\sin\alpha_2)\sin\phi\right. \end{aligned}$$

$$V_{03} = -\tfrac{1}{2}\left\{(V_{S2}+V_{S3}) - \left[\left(V_{S2}^2 + V_{S3}^2\right) - 2V_{S2}V_{S3}\cos(\alpha_2-\alpha_3)\right]^{\frac{1}{2}}\right\}$$

Mass Flow Rates

$$M = \frac{pV}{RT}$$

$$\dot{M} = \left(\frac{dM}{d\phi}\right)\frac{d\phi}{dt}$$

$$\dot{M} = \left(\frac{1}{RT}\right)\left[V\frac{dp}{d\phi} + p\frac{dv}{d\phi}\right]\frac{d\phi}{dt}$$

$$\frac{d\phi}{dt} = 2\pi N \qquad (N = \text{rotational speed (r.p.s.)})$$

$$\dot{M} = \frac{2\pi N}{RT}\left[V\frac{dp}{d\phi} + p\frac{dv}{d\phi}\right]$$

$$p = \frac{p_{max}(1-\delta)}{\left[1+\delta\cos(\phi-\theta)\right]}$$

$$\dot{M} = \left(\frac{2\pi N}{RT}\right)\left[\frac{p_{max}(1-\delta)}{1+\delta\cos(\phi-\theta)}\right]\left\{\frac{V\delta\sin(\phi-\theta)}{\left[1+\delta\cos(\phi-\theta)\right.} + \frac{dv}{d\phi}\right\}$$

$$\frac{dv_1}{d\phi} = \frac{1}{2}v_{s1}\sin\phi$$

$$\frac{dv_2}{d\phi} = -\frac{1}{2}v_{s1}\sin\phi + \frac{1}{2}v_{s2}\sin(\phi-\alpha_2) + \frac{dv_{o2}}{d\phi}$$

$$\frac{dv_3}{d\phi} = -\frac{1}{2}v_{s2}\sin(\phi-\alpha_2) + \frac{1}{2}v_{s3}\sin(\phi-\alpha_3) + \frac{dv_{o3}}{d\phi}$$

Beta Stirling Engine/Heat Pump Analysis

TABLE D1

Input Data:

Piston Dia [cm]	=	5.00		
x1, x2, x3 [cm]	=	10.00	10.00	10.00
Vd1, Vd2, Vd3 [cc]	=	150.00	150.00	150.00
Vo2, Vo3 [cc]	=	0.00	0.00	
alpha2, alpha3 [deg]	=	150.00	100.00	
T1, T2, T3 [K]	=	1000.00	500.00	300.00
Pmax [atm]	=	10.00		
Molecular Weight of gas	=	29.00		
$\Delta\phi$ [deg]	=	30.00		
Rotational Speed [rpm]	=	10.00		

Results:

Volumes [cc]:

Vs1 =	196.35
Vs2 =	196.35
Vs3 =	196.35

Work [Joules/cycle]:

W1 =	-33.94
W2 =	60.58
W3 =	-26.17
Wt =	0.47

Pressures, Volumes, and Mass Flow Rates:

ϕ [deg]	Pressure [atm]	V1 (swept) [cc]	V2 (swept) [cc]	V3 (swept) [cc]	$\dot{M}$ 1 [gm/s]	$\dot{M}$ 2 [gm/s]	$\dot{M}$ 3 [gm/s]	$\dot{M}$ d1 [gm/s]	$\dot{M}$ d2 [gm/s]	$\dot{M}$ d3 [gm/s]	$\dot{M}$r12 [gm/s]	$\dot{M}$r23 [gm/s]
0	8.59	0.00	379.55	128.38	0.0000	-0.0221	-0.3408	0.0573	0.1146	0.1910	-0.0573	-0.1498
30	9.16	13.15	330.46	113.68	0.1719	-0.6373	0.0743	0.0618	0.1235	0.2059	-0.2336	0.2802
60	9.69	49.09	245.44	121.14	0.3202	-1.1612	0.5450	0.0467	0.0934	0.1557	-0.3669	0.7008
90	9.98	98.17	147.26	148.75	0.3709	-1.3289	0.8785	0.0125	0.0251	0.0418	-0.3834	0.9203
120	9.91	147.26	62.24	189.12	0.2849	-1.0063	0.8952	-0.0274	-0.0549	-0.0914	-0.2574	0.8038
150	9.50	183.20	13.15	231.42	0.1054	-0.3550	0.5985	-0.0551	-0.1102	-0.1836	-0.0503	0.4149
180	8.94	196.35	13.15	264.32	-0.0812	0.3138	0.1603	-0.0620	-0.1241	-0.2068	0.1432	-0.0465
210	8.39	183.20	62.24	279.01	-0.2156	0.7897	-0.2462	-0.0518	-0.1036	-0.1726	0.2674	-0.4188
240	7.99	147.26	147.26	271.56	-0.2826	1.0210	-0.5373	-0.0318	-0.0635	-0.1059	0.3143	-0.6432
270	7.80	98.17	245.44	243.95	-0.2885	1.0329	-0.6958	-0.0077	-0.0153	-0.0256	0.2962	-0.7214
300	7.85	49.09	330.46	203.58	-0.2413	0.8548	-0.7224	0.0172	0.0344	0.0573	0.2241	-0.6651
330	8.12	13.15	379.55	161.28	-0.1440	0.4986	-0.6093	0.0402	0.0804	0.1341	0.1038	-0.4752
360	8.59	0.00	379.55	128.38	-0.0000	-0.0221	-0.3408	0.0573	0.1146	0.1910	-0.0573	-0.1498